

8527

NACA TN 2101

0065398



TECH LIBRARY KAFB, NM

# NATIONAL ADVISORY COMMITTEE FOR AERONAUTICS

TECHNICAL NOTE 2101

A NUMERICAL PROCEDURE FOR DESIGNING CASCADE BLADES  
WITH PRESCRIBED VELOCITY DISTRIBUTIONS  
IN INCOMPRESSIBLE POTENTIAL FLOW

By Arthur G. Hansen and Peggy L. Yohner

Lewis Flight Propulsion Laboratory  
Cleveland, Ohio



Washington

June 1950

AFMTC  
TECHNICAL NOTE  
AFL 2511

317.98/40



## NATIONAL ADVISORY COMMITTEE FOR AERONAUTICS

## TECHNICAL NOTE 2101

A NUMERICAL PROCEDURE FOR DESIGNING CASCADE BLADES WITH PRESCRIBED  
VELOCITY DISTRIBUTION IN INCOMPRESSIBLE POTENTIAL FLOW

By Arthur G. Hansen and Peggy L. Yohner

## SUMMARY

A step-by-step numerical procedure based on a conformal-mapping theory is presented for the design of a cascade of airfoils with a prescribed dimensionless-velocity distribution in incompressible potential flow. The numerical procedure includes a set of tables to serve as a guide in computation. A numerical example is also presented in order to illustrate specific solutions to some of the more difficult problems arising in the design of a cascade by this method.

The conjugate harmonic function was evaluated by use of the method outlined by Naiman. Two separate calculations were made: one used 360 equally spaced values of the circle angle  $\theta$ , and the other used 90 equally spaced values of  $\theta$ . The 90-point method did not insure sufficient accuracy for the example used. The accuracy, however, depends on the design conditions prescribed and, consequently, it cannot be inferred that the 90-point method will give inaccurate results in all cases.

## INTRODUCTION

Several exact solutions to the problem of obtaining an airfoil cascade in incompressible potential flow with a prescribed velocity distribution on an airfoil in the cascade have been obtained by the method of conformal transformation (references 1 to 3). The numerical computations involved in conformal-mapping methods are, however, usually quite long and complicated. A detailed numerical procedure that is intended to make the actual application of a conformal-mapping method to cascade design more efficient in regard to time and personnel was therefore developed at the NACA Lewis laboratory and is presented herein.

The procedure employed requires the specification of the dimensionless-velocity distribution on an airfoil in the cascade

and the values of the upstream and downstream velocity vectors of the flow through the cascade. The velocity distribution specified for an airfoil may not be theoretically attainable; that is, the airfoil profiles calculated by use of this velocity distribution would not have closed contours. It is possible, however, to modify the velocity distribution in such a manner that closed profiles will result.

A numerical example is included with the procedure in order to illustrate specific solutions to some of the more difficult problems arising in the design of a cascade by this method. A brief summary of the theory underlying the numerical procedure is presented to acquaint the reader with the fundamental principles employed in the solution of the problem. More detailed discussions of the theory are presented in references 1 to 3.

### SYMBOLS

The following symbols are used in this report:

$C$	constant
$d$	dimensionless spacing of airfoils in cascade (ratio of actual spacing to prescribed suction-surface arc length)
$f(\theta)$	function added to $p(\theta)$ to satisfy conditions on $h(z)$
$h(z)$	analytic function of $z$
$k$	constant locating complex sources in $z$ -plane
$N$	constant determining amplitude of sine curve
$p(x,y)$	harmonic function
$p'(\theta)$	$p(\theta) + f(\theta)$ corrected harmonic function
$Q(z)$	function of $z$ defined by equation (11)
$q(x,y)$	conjugate harmonic function of $p(x,y)$
Re	"real part of"
$S$	dimensionless airfoil arc length (ratio of actual arc length to suction-surface arc length)

$S'$	corrected dimensionless airfoil arc length (ratio of corrected arc length to prescribed suction-surface arc length)
$S_{T,1}, S_{T,2}$	value of $S$ corresponding to trailing edge of airfoil when approached from pressure and suction surfaces, respectively
$u(S)$	airfoil velocity function (equation (4))
$u'$	corrected value of $u$
$V$	magnitude of dimensionless velocity vector (ratio of actual velocity to maximum airfoil velocity)
$v$	magnitude of prescribed dimensionless airfoil velocity (ratio of actual velocity to maximum airfoil velocity)
$v'$	corrected value of $v$
$v_c(\theta)$	velocity on unit circle
$W=\phi+i\psi$	complex potential function
$z=x+iy$ ,	complex variable denoting circle plane
$\alpha$	constant determining phaseangle of sine curve
$\beta(\theta)$	function of $\theta$ defined by equation (25)
$\Gamma$	circulation (positive counterclockwise)
$\gamma$	constant determining wave length of sine curve
$\Delta$	velocity-potential range on airfoil
$\Delta_k$	velocity-potential range on unit circle
$\epsilon$	included trailing-edge angle of airfoil
$\zeta=\xi+i\eta$ ,	complex variable denoting cascade plane (equations (23) and (24))
$\theta$	circle angle ( $z$ -plane)
$\theta_1$	particular value of $\theta$

$\phi$	velocity potential
$\lambda$	angle of velocity vector (positive clockwise)
$\lambda_k$	auxiliary constant defined by equation (28)
$\psi$	stream function

## Subscripts:

a	cascade plane
c	circle plane
j	indicates particular values of $N$ , $\gamma$ , and $\alpha$
m	mean flow conditions
N	leading edge (nose)
T	trailing edge (tail)
1	upstream
2	downstream
3	} various constants
4	
5	
6	
7	

A function of  $(z = x + iy)$  or of  $(x,y)$  expressed as a function of  $\theta$  implies that the function is evaluated for  $z = e^{i\theta}$ .

## REVIEW OF BASIC THEORY

The solution to the problem of designing a cascade by the method to be outlined is based on conformal-mapping techniques similar to those employed in references 1 to 3. The desired cascade of airfoils is determined by forming an analytic function of a complex variable, which effects a mapping of the incompressible potential flow about a unit circle into the incompressible potential flow about the cascade. The mapping function is such that the unit circle is thereby transformed into the airfoils of the cascade.

The numerical solution involves two problems: (1) the determination of the potential flow about the unit circle; and (2) the determination of the mapping function and the airfoil coordinates. Before these problems can be solved, however, the following design information must be specified:

1. The magnitude of the dimensionless velocity  $v$  along an airfoil in the cascade, as a function of the dimensionless airfoil arc length  $S$

The dimensionless arc length  $S$  will be considered negative from  $S_{T,1}$  to zero, and positive from zero to  $S_{T,2}$ , where  $S_{T,1}$  and  $S_{T,2}$  represent the trailing-edge stagnation point on an airfoil when approached from the pressure and suction surfaces, respectively. The leading-edge stagnation points correspond to  $S = 0$  (fig. 1).

2. The upstream and downstream dimensionless velocity vectors of the flow through the cascade

These vectors will be designated  $V_1 e^{-i(\lambda_1 - \pi)}$  and  $V_2 e^{-i(\lambda_2 - \pi)}$ , respectively, where  $V_1$  and  $V_2$  are the magnitudes of these velocities and  $\lambda_1$  and  $\lambda_2$  are the directions (positive clockwise) of the velocities as measured from a line perpendicular to the cascade axis (fig. 2). The four quantities  $V_1$ ,  $V_2$ ,  $\lambda_1$ , and  $\lambda_2$  cannot be specified independently, however, as they must satisfy the continuity equation

$$V_1 \cos \lambda_1 = V_2 \cos \lambda_2$$

#### Determination of Complex Potential Function in Circle Plane

In this discussion of the solution of each of the previously mentioned problems, the complex plane containing the cascade is designated the  $\xi = (\xi + i\eta)$  plane or cascade plane; whereas the complex plane containing the unit circle is designated the  $z = x + iy$  plane or circle plane.

The complex potential function  $W_o(z)$  for the flow in the circle plane due to complex sources located at  $z = \pm e^{\pm k}$  (reference 4, notation modified) is given as

$$W_c(z) = \frac{V_m d}{2\pi} \left[ e^{i\lambda_m} \log_e \left( \frac{z - e^k}{z + e^k} \right) + e^{-i\lambda_m} \log_e \left( \frac{z - e^{-k}}{z + e^{-k}} \right) \right] + \frac{\Gamma}{4\pi i} \log_e \left( \frac{z^2 - e^{-2k}}{z^2 - e^{2k}} \right) + C_3 \quad (1)$$

It is evident that equation (1) will be specifically determined when the constants  $k$ ,  $V_m$ ,  $\lambda_m$ ,  $d$ , and  $\Gamma$  are known. The constants  $V_m$ ,  $\lambda_m$ ,  $d$ , and  $\Gamma$  can be determined directly from the prescribed velocity distribution for the airfoils in the cascade and the upstream and downstream velocities of the flow through the cascade. Specifically,

$$\lambda_m = \tan^{-1} \left( \frac{\tan \lambda_1 + \tan \lambda_2}{2} \right) \quad (2)$$

where

$$-\frac{\pi}{2} < \lambda_m < \frac{\pi}{2}$$

$$V_m = \frac{V_1 \cos \lambda_1}{\cos \lambda_m} \quad (3)$$

$$\Gamma = \int_{S_{T,1}}^{S_{T,2}} u(s) \, ds \quad (4)$$

where

$$u(s) = -v(s) \quad \text{for } S_{T,1} \leq s \leq 0$$

$$u(s) = v(s) \quad \text{for } 0 < s \leq S_{T,2}$$

( $v(S)$ ) is the prescribed velocity as a function of  $S$

$$d = \frac{\Gamma}{(v_1 \sin \lambda_1 - v_2 \sin \lambda_2)} \quad (5)$$

The constant  $k$  is determined by the condition that the range of the velocity potential (the difference between the maximum and minimum values of the velocity potential) on an airfoil must equal the range of the velocity potential on the unit circle.

The velocity potential on an airfoil  $\varphi_a(S)$  can be determined from the equation

$$\varphi_a(S) = \int_{S_{T,1}}^S u(S) dS \quad (6)$$

The velocity-potential range  $\Delta$  on an airfoil is then

$$\Delta = \varphi_a(S_{T,2}) - \varphi_a(0) \quad (7)$$

The velocity potential on the unit circle  $z = e^{i\theta}$  is given by

$$\varphi_c(\theta) = \text{Re} \left[ W(e^{i\theta}) \right] \quad (8)$$

where the constant  $C_3$  in equation (1) has been so chosen that  $\varphi_c(\theta)$  is zero for the value of  $\theta$  corresponding to the trailing-edge stagnation point on the circle. Then the velocity-potential range on the circle  $\Delta_k$  for a given value of  $k$  is

$$\Delta_k = \varphi_c(\theta_T + 2\pi) - \varphi_c(\theta_N) \quad (9)$$

where  $\theta_T$  and  $\theta_N$  are the values of  $\theta$  corresponding to the trailing- and leading-edge stagnation points on the circle, respectively.

It is possible to find  $k$  (and also  $\theta_T$  and  $\theta_N$ ) by a process of trial and error so that  $\Delta = \Delta_k$ . (See section NUMERICAL PROCEDURE.)



# Determination of Mapping Function and Airfoil Coordinates

8

The general form of a mapping function that effects the desired transformation between the  $\zeta$ -plane and the  $z$ -plane is given by

$$\frac{d\zeta}{dz} = \frac{de^{-k}}{\pi} \left(1 - \frac{z_T}{z}\right)^{1 - \frac{\epsilon}{\pi}} \left(1 - \frac{z_T^2}{e^{2k} z^2}\right)^{-\frac{1}{2} + \frac{\epsilon}{2\pi}} Q(z) e^{\frac{h(z)}{Q(z)}} \exp \left[ \frac{e^k \left(\frac{1}{2} - \frac{\epsilon}{2\pi}\right)}{z} \log_e \frac{e^k + z_T}{e^k - z_T} \right] \quad (10)$$

where

$\epsilon$  specified included trailing-edge angle of airfoils in cascade (for example,  $\epsilon = 0$  for cusped tails,  $\epsilon = \pi$  for rounded tails)

$$Q(z) = \frac{z^2 (e^{2k} - e^{-2k})}{(e^{2k} - z^2)(z^2 - e^{-2k})} \quad (11)$$

and

$$h(z) = p(x,y) + iq(x,y)$$

is a complex function, analytic and single-valued for  $|z| > 1$ , and is such that

$$\lim_{z \rightarrow \infty} zh(z) = 0 \quad (12)$$

It is seen from equation (10) that the mapping function is specifically determined if the analytic function  $h(z) = p(x,y) + iq(x,y)$  is known. Actually, the process of obtaining the coordinates of an airfoil in the cascade requires only that  $d\zeta/dz$  be known for values

of  $z$  on the unit circle. It is therefore sufficient to evaluate  $h(e^{i\theta}) = p(\theta) + iq(\theta)$  in order to accomplish this result.

Evaluation of  $p(\theta)$  and  $q(\theta)$ . - A condition that holds between the cascade plane and the circle plane is

$$\varphi_a(\xi) + i\psi_a(\xi) = W_c(z) \quad (13)$$

where  $\varphi_a$  and  $\psi_a$  are the velocity potential and the stream function, respectively, for the flow in the cascade plane. From this relation it is possible to deduce that

$$\frac{v_c(\theta)}{u(\theta)} = \left| \left( \frac{d\xi}{dz} \right)_{z=e^{i\theta}} \right| \quad (14)$$

where

$$v_c(\theta) = \operatorname{Re} \left[ \frac{dW_c(z)}{dz} \right]_{z=e^{i\theta}} \quad (15)$$

is the velocity on the unit circle and  $u(\theta) \equiv u(S)$  as a function of  $\theta$ .

From equations (10) and (14) is obtained

$$\frac{v_c(\theta)}{u(\theta)} = \frac{dQ(\theta)}{\pi \left[ 2 \sin \left( \frac{\theta - \theta_T}{2} \right) \right]^{\frac{\epsilon}{\pi} - 1}} \exp \left\{ \frac{p(\theta)}{Q(\theta)} - k - \left( \frac{1}{2} - \frac{\epsilon}{2\pi} \right) \left[ \log_e \sqrt{2 (\cosh 2k - \cos 2\theta_T)} - \right. \right. \\ \left. \left. k - e^k \cos \theta \tanh^{-1} \left( \frac{\cos \theta_T}{\cosh k} \right) - e^k \sin \theta \tanh^{-1} \left( \frac{\sin \theta_T}{\sinh k} \right) \right] \right\} \quad (16)$$

Equation (16) can now be solved for  $p(\theta)$ ,

$$p(\theta) = Q(\theta) \left( \log_e \left\{ \frac{\pi}{dQ(\theta)} \frac{v_c(\theta)}{u(\theta)} \left[ 2 \sin \left( \frac{\theta - \theta_T}{2} \right) \right]^{\frac{\epsilon}{\pi} - 1} \right\} + \right. \\ \left. k + \left( \frac{1}{2} - \frac{\epsilon}{2\pi} \right) \left[ \log_e \sqrt{2 (\cosh 2k - \cos 2\theta_T)} - k - \right. \right. \\ \left. \left. e^k \cos \theta \tanh^{-1} \left( \frac{\cos \theta_T}{\cosh k} \right) - e^k \sin \theta \tanh^{-1} \left( \frac{\sin \theta_T}{\sinh k} \right) \right] \right) \quad (17)$$

where

$$-\frac{\pi}{2} \leq \tanh^{-1} \left( \frac{\sin \theta_T}{\sinh k} \right) \leq \frac{\pi}{2}$$

All quantities in equation (17) have been previously evaluated except  $u(\theta)$ . The procedure for evaluating  $u(\theta)$  is as follows: From equations (8) and (13) the relation

$$\varphi_a(S) = \varphi_c(\theta) \quad (18)$$

is obtained for corresponding values of  $S$  and  $\theta$ . By matching these velocity potentials,  $S$  can be obtained as a function of  $\theta$  and, consequently,  $u(S)$  can be obtained as a function of  $\theta$ ,  $u(\theta)$ . Hence,  $p(\theta)$  can be evaluated from equation (17).

The necessary and sufficient condition that the condition imposed on the function  $h(z)$  by equation (12) is satisfied is

$$\int_{\theta_T}^{\theta_T + 2\pi} p(\theta) d\theta = \int_{\theta_T}^{\theta_T + 2\pi} p(\theta) \sin \theta d\theta = \int_{\theta_T}^{\theta_T + 2\pi} p(\theta) \cos \theta d\theta = 0$$

Usually the values of these integrals will not be zero and, consequently, a correction term  $f(\theta)$  must be added to  $p(\theta)$  such that if

$$p'(\theta) = p(\theta) + f(\theta)$$

Then

$$\int_{\theta_T}^{\theta_T + 2\pi} p'(\theta) d\theta = \int_{\theta_T}^{\theta_T + 2\pi} p'(\theta) \sin \theta d\theta = \int_{\theta_T}^{\theta_T + 2\pi} p'(\theta) \cos \theta d\theta = 0 \quad (19)$$

If it is assumed that the values of the integrals involving  $p(\theta)$  are not zero, but instead are

$$\int_{\theta_T}^{\theta_T + 2\pi} p(\theta) d\theta = C_4$$

$$\int_{\theta_T}^{\theta_T + 2\pi} p(\theta) \sin \theta d\theta = C_5$$

$$\int_{\theta_T}^{\theta_T + 2\pi} p(\theta) \cos \theta d\theta = C_6$$

it follows that  $f(\theta)$  must be a function such that

$$\int_{\theta_T}^{\theta_T + 2\pi} f(\theta) d\theta = -C_4$$

$$\int_{\theta_T}^{\theta_T + 2\pi} f(\theta) \sin \theta d\theta = -C_5$$

$$\int_{\theta_T}^{\theta_T + 2\pi} f(\theta) \cos \theta d\theta = -C_6$$

The proper choice of  $f(\theta)$  fulfilling these requirements is somewhat arbitrary. The addition of  $f(\theta)$  to  $p(\theta)$  will, however, produce a change in the prescribed airfoil velocity and the prescribed arc length on the airfoil for  $\theta_T \leq \theta \leq \theta_T + 2\pi$ , given by

$$\left. \begin{aligned} v'(\theta) &= -u(\theta)e^{-f(\theta)/Q(\theta)} \text{ for } \theta_T \leq \theta \leq \theta_N \\ v'(\theta) &= u(\theta)e^{-f(\theta)/Q(\theta)} \text{ for } \theta_N \leq \theta \leq \theta_T + 2\pi \end{aligned} \right\} \quad (20)$$

and

$$S'(\theta) = \int_{\theta_N}^{\theta} e^{f(\theta)/Q(\theta)} \frac{dS(\theta)}{d\theta} d\theta \quad (21)$$

These equations are the parametric equations for  $v'(S')$  where  $v'(S')$  represents the corrected airfoil velocity as a function of corrected arc length. It is possible in many instances, however, to prescribe  $f(\theta)$  in such a manner that it is zero for values of  $\theta$  corresponding to certain regions of the airfoil, such as the suction surface. Over these regions, the magnitude of the prescribed velocity as a function of  $\theta$  will remain unaltered.

The function  $q(\theta)$  can be evaluated for various values of  $\theta$  from the equation

$$q(\theta_1) = \int_{\theta_T}^{\theta_T + 2\pi} p(\theta) \cot\left(\frac{\theta - \theta_1}{2}\right) d\theta \quad (22)$$

where  $\theta_1$  is a particular value of  $\theta$ . The function  $p(\theta)$  in this equation is replaced by  $p'(\theta)$  if  $p(\theta)$  has been corrected.

Determination of airfoil coordinates. - The coordinates  $(\xi, \eta)$  of an airfoil in the cascade can be obtained in the following manner: The complex variable  $\zeta = \xi + i\eta$  can be expressed as

$$\zeta = \int dz = \int \frac{d\zeta}{dz} dz$$

The real and imaginary parts of  $\int \frac{dz}{z}$  for  $z = e^{i\theta}$  now give the coordinates  $\xi$  and  $\eta$ , respectively, of the airfoil. Specifically, for  $p(\theta)$  uncorrected,

$$\xi = \int \left| \frac{dz}{z} \right| \cos \beta(\theta) d\theta = \int \frac{v_c(\theta)}{u(\theta)} \cos \beta(\theta) d\theta \quad (23)$$

$$\eta = \int \left| \frac{dz}{z} \right| \sin \beta(\theta) d\theta = \int \frac{v_c(\theta)}{u(\theta)} \sin \beta(\theta) d\theta \quad (24)$$

where

$$\begin{aligned} \beta(\theta) &= \frac{\pi}{2} + \theta + \arg \left( \frac{dz}{z} \right)_{z=e^{i\theta}} \\ &= \frac{q(\theta)}{Q(\theta)} + \left(1 - \frac{\epsilon}{\pi}\right) \left\{ \frac{\pi}{2} - \frac{\theta}{2} + \frac{1}{2} \tan^{-1} \left( \frac{\tan \theta_T}{\tanh k} \right) + \right. \\ &\quad \left. \frac{e^k}{2} \left[ \cos \theta \tan^{-1} \left( \frac{\sin \theta_T}{\sinh k} \right) - \sin \theta \tanh^{-1} \left( \frac{\cos \theta_T}{\cosh k} \right) \right] \right\} + \theta + \frac{\pi}{2} \quad (25) \end{aligned}$$

and where  $\tan^{-1} \left( \frac{\tan \theta_T}{\tanh k} \right)$  is in the same quadrant and has the same sign as  $\theta_T$ .

If the function  $p(\theta)$  has been corrected, the following equations are used in place of equations (23) and (24):

$$\xi = \int \frac{v_c(\theta)}{u'(\theta)} \cos \beta(\theta) d\theta \quad (26)$$

$$\eta = \int \frac{v_c(\theta)}{u'(\theta)} \sin \beta(\theta) d\theta \quad (27)$$

### Restrictions on Airfoil Velocity for Specified Trailing-edge Angles

It can be shown from equation (17) that the function  $u(\theta)$  must possess the following properties for cusped-, rounded-, or pointed-trailing-edge airfoils:

1. Cusped trailing edge:  $-u(\theta_T) = +u(\theta_T + 2\pi) = C$ , where  $C$  is a positive constant
2. Rounded trailing edge:  $u(\theta_T) = u(\theta_T + 2\pi) = 0$ , where the zero is of order of one
3. Pointed trailing edge (trailing-edge angle  $= \epsilon$ ):  $u(\theta_T) = u(\theta_T + 2\pi) = 0$ , where the zero is of order of  $\epsilon/\pi$ .

As there is no convenient method of determining from  $u(S)$  the behavior of  $u(\theta)$  at  $\theta_T$  and  $\theta_T + 2\pi$  before extensive calculations have been performed, it may be necessary to modify  $u(\theta)$  to fulfill the preceding conditions. This modification will result in a slight change in  $u(S)$  at  $S_{T,1}$  and  $S_{T,2}$ . An approximation to the preceding conditions on  $u(\theta)$  can be made, however, by applying the restrictions to  $u(S)$  at  $S_{T,1}$  and  $S_{T,2}$ .

### NUMERICAL PROCEDURE

The numerical procedure that follows will list the computational steps leading to the evaluation of the coordinates of an airfoil in the cascade. These steps have been included in a set of tables to serve as a guide in performing numerical computations. The two problems previously mentioned - namely, the determination of the complex potential function in the circle plane, and the determination of the mapping function and the airfoil coordinates - will be treated separately.

#### Determination of Complex Potential Function in Circle Plane

The complex potential function  $W(z)$  (equation (1)) can be determined if the constants  $\lambda_m$ ,  $V_m$ ,  $\Gamma$ ,  $d$ , and  $k$  are known.

Evaluation of  $\lambda_m$ ,  $V_m$ ,  $\Gamma$ , and  $d$ . - The constants  $\lambda_m$ ,  $V_m$ ,  $\Gamma$ , and  $d$  are evaluated from equations (2), (3), (4), and (5), respectively.

Evaluation of  $k$ . - The constant  $k$  is evaluated by a process of trial and error that simultaneously determines  $\theta_N$  and  $\theta_T$ . The procedure required to evaluate these constants is:

1. Determine the velocity-potential range  $\Delta$  on an airfoil in the cascade from equation (7).
2. Assume a value of  $k$  (probably between 0 and 1) and determine the auxiliary constant

$$\lambda_k \equiv \tan^{-1} (\tan \lambda_m \tanh k) \quad (28)$$

where

$$-\frac{\pi}{2} < \lambda_k < \frac{\pi}{2}$$

3. Determine  $\theta_N$  and  $\theta_T$  from the following equations. (reference 4):

$$\theta_N + \lambda_k = \sin^{-1} \left( \frac{-\Gamma}{2V_m d} \frac{\cosh k \sin \lambda_k}{\sin \lambda_m} \right) \quad (29)$$

$$-\frac{\pi}{2} < \theta_N + \lambda_k < \frac{\pi}{2}$$

$$\theta_T = -\theta_N - \pi - 2\lambda_k \quad (30)$$

4. Calculate the velocity potential range on the unit circle for the assumed value of  $k$  from



$$\Delta_k = \varphi_c(\theta_T + 2\pi) - \varphi_c(\theta_N) \quad (9)$$

$$= \frac{V_{m^d}}{\pi} \left\{ \sin \lambda_m \left[ \tan^{-1} \left( \frac{\sin \theta_T}{\sinh k} \right) - \tan^{-1} \left( \frac{\sin \theta_N}{\sinh k} \right) \right] - \right. \\ \left. \cos \lambda_m \left[ \tanh^{-1} \left( \frac{\cos \theta_T}{\cosh k} \right) - \tanh^{-1} \left( \frac{\cos \theta_N}{\cosh k} \right) \right] + \right. \\ \left. \frac{\Gamma}{2V_{m^d}} \left[ \tan^{-1} \left( \frac{\tan \theta_T}{\tanh k} \right) + 2\pi - \tan^{-1} \left( \frac{\tan \theta_N}{\tanh k} \right) \right] \right\}$$

where

$$-\frac{\pi}{2} < \tan^{-1} \left( \frac{\sin \theta_T}{\sinh k} \right) < \frac{\pi}{2}$$

$$-\frac{\pi}{2} < \tan^{-1} \left( \frac{\sin \theta_N}{\sinh k} \right) < \frac{\pi}{2}$$

and  $\tan^{-1} \left( \frac{\tan \theta_T}{\tanh k} \right)$  and  $\tan^{-1} \left( \frac{\tan \theta_N}{\tanh k} \right)$  are in the same quadrant and have the same sign as  $\theta_T$  and  $\theta_N$ , respectively.

5. Repeat steps (1) to (4), assuming several new values for  $k$  until, by interpolation or plotting  $\Delta_k$  against  $k$ , a value of  $k$  can be found such that  $\Delta_k = \Delta$ . The correct values of  $k$ ,  $\theta_T$ , and  $\theta_N$  are those that produce this last equality. (The evaluation of  $k$  is given in table I.)

#### Determination of Mapping Function and Airfoil Coordinates

The mapping function will be determined on the unit circle if the functions  $p(\theta)$  and  $q(\theta)$  are known. The airfoil coordinates can then be obtained from the mapping function.

Determination of  $p(\theta)$ . -

1. Evaluate the velocity on the unit circle for  $(\theta_T \leq \theta \leq \theta_T + 2\pi)$

$$v_c(\theta) = \operatorname{Re} \left[ \frac{dW_c(z)}{dz} \right]_{z=e^{i\theta}} \quad (15)$$

$$= \frac{V_{m^d}}{\pi} \frac{\sin \lambda_m Q(\theta) [\sin(\theta + \lambda_k) - \sin(\theta_T + \lambda_k)]}{\sin \lambda_k \cosh k}$$

where  $Q(\theta)$  is given by

$$Q(\theta) = \frac{\sinh 2k}{\cosh 2k - \cos 2\theta} = \frac{\sinh k \cosh k}{\sinh^2 k \sin^2 \theta}$$

(The evaluation of  $v_c(\theta)$  is given in columns 1 to 9 in table II)

2. Evaluate  $u(\theta)$  in the following manner:

Plot  $\varphi_a(S)$  (equation (6)) and evaluate  $\varphi_c(\theta)$  from  $\theta_T \leq \theta \leq \theta_T + 2\pi$ , where

$$\varphi_c(\theta) = \operatorname{Re} [W(e^{i\theta})] \quad (8)$$

$$= \frac{V_{m^d}}{\pi} \left\{ \left[ \sin \lambda_m \tan^{-1} \left( \frac{\sin \theta}{\sinh k} \right) - \cos \lambda_m \tanh^{-1} \left( \frac{\cos \theta}{\cosh k} \right) \right] + \right.$$

$$\left. \frac{\Gamma}{2V_{m^d}} \tan^{-1} \left( \frac{\tan \theta}{\tanh k} \right) \right\} + C_7$$

where  $C_7$  is a constant such that  $\varphi_c(\theta_T) = 0$  and

$$-\frac{\pi}{2} < \tan^{-1} \left( \frac{\sin \theta}{\sinh k} \right) < \frac{\pi}{2}$$

The term  $\tan^{-1} \left( \frac{\tan \theta}{\tanh k} \right)$  is in the same quadrant and has the same sign as  $\theta$ . (The evaluation of  $\varphi_c(\theta)$  is given in columns 10 to 24 in table II.)

Beginning at the point  $S_{T,1}$  on the airfoil velocity-potential curve and at the point  $\theta_T$  on the circle velocity-potential curve, progressively match the values of  $\varphi_a(S)$  and  $\varphi_c(\theta)$  from  $S_{T,1}$  and  $\theta_T$  to  $S_{T,2}$  and  $\theta_T + 2\pi$ , thereby establishing a one-to-one correspondence between the values of  $\theta$  and  $S$ , which satisfies

$$\varphi_a(S) = \varphi_c(\theta) \quad (18)$$

As  $S(\theta)$  is known,  $u(S)$  is obtained as a function of  $\theta$ ,  $u(\theta)$ .

3. The function  $p(\theta)$  is now determined from equation (17) (The evaluation of  $p(\theta)$  is given in columns 25 to 38 of table II.)

Correction of  $p(\theta)$  to satisfy conditions on  $h(z)$ . - Compute (by numerical integration) the integrals

$$\int_{\theta_T}^{\theta_T + 2\pi} p(\theta) d\theta$$

$$\int_{\theta_T}^{\theta_T + 2\pi} p(\theta) \sin \theta d\theta$$

$$\int_{\theta_T}^{\theta_T + 2\pi} p(\theta) \cos \theta d\theta$$

as indicated in columns 39 to 43 in table II.

If these integrals are not zero, form the function  $p'(\theta) = p(\theta) + f(\theta)$  where  $p'(\theta)$  and  $f(\theta)$  fulfill the conditions of equation (19) (columns 44 to 50 of table II). One expression for  $f(\theta)$  is given by

$$f(\theta) = N_1 \sin \gamma_1 (\theta + \alpha_1) + N_2 \sin \gamma_2 (\theta + \alpha_2) + N_3 \sin \gamma_3 (\theta + \alpha_3) \quad (31)$$

for

$$\left(-\alpha_j - \frac{\pi}{\gamma_j}\right) \leq \theta \leq -\alpha_j$$

where  $j = 1, 2, 3$  in the term that has the subscript corresponding to  $j$ ;  $f(\theta) = 0$  for all other values of  $\theta$ .

The constants  $N_j$ ,  $\gamma_j$ , and  $\alpha_j$  ( $j = 1, 2, 3$ ) are chosen so as to fulfill the integral requirements and, if possible, restrict the velocity change to a minimum. It seems advisable in this case to assume various values for  $\gamma_j$  and  $\alpha_j$  and to evaluate  $N_j$  from the integral requirements.

Determination of  $q(\theta)$ . - The function  $q(\theta)$  is evaluated from equation (22) either by some form of numerical integration or by the method of Naiman (reference 6).

Determination of airfoil coordinates. -

1. Evaluate  $\beta(\theta)$  from equation (25). (The evaluation of  $\beta(\theta)$  is given in columns 51 to 64 in table II.)
2. Evaluate the airfoil coordinates from equations (23) and (24) if  $p(\theta)$  has not been corrected, or from equations (26) and (27) if  $p(\theta)$  has been corrected. (The airfoil coordinates are evaluated in columns 65 to 71 in table II.)

#### APPLICATION OF NUMERICAL PROCEDURE

Several important problems arise in the application of the numerical procedure to the design of a particular cascade. These problems may be listed as follows:

1. The number of values of  $\theta$  to be chosen for computations
2. The method of selecting functions to add to  $p(\theta)$  in order to satisfy conditions on  $h(z)$
3. The method of evaluating  $q(\theta)$  from equation (22)
4. The type of numerical integration to be used in evaluating the various integrals that appear in the procedure

The solutions to these problems of the numerical techniques to be employed to give a certain accuracy in computations will depend largely on the particular design being considered. At present, no general solutions can be given.

In order to illustrate particular solutions to these problems, however, and to clarify the numerical procedure, a cascade of airfoils with cusped tails was computed. It was decided in advance to compute an airfoil in the cascade in two ways. One method was to use 360 equally spaced values of  $\theta$  and the other was to use 90 equally spaced values of  $\theta$ . The choice of the number of values of  $\theta$  was made in order to investigate the accuracy of using the method of Naiman (reference 6) in computing the values of  $q(\theta)$  for the problem chosen and to investigate further the influence of this accuracy on the computed airfoil coordinates. The values of  $\theta$  had to be equally spaced to use Naiman's method for computing  $q(\theta)$ . Naiman's method had particularly been chosen for the evaluation of  $q(\theta)$  because of its applicability to calculation by punch-card machines. In all calculations where numerical integration was required, Simpson's 1/3, or parabolic method, was used because it was felt that this method would give sufficient accuracy for the values of  $\theta$  chosen. In all numerical work, five significant figures were used, as it was believed this accuracy was sufficient for the example.

#### Design Specifications

The velocity on an airfoil in the cascade was expressed non-dimensionally as the ratio of the actual airfoil velocity to the maximum airfoil velocity. The airfoil arc length was expressed non-dimensionally as the ratio of the actual airfoil arc length to the total airfoil suction-surface arc length. The velocity distribution is shown in figure 3.

The magnitudes of the inlet and exit velocity vectors were chosen as, respectively,

$$V_1 = 0.68229$$

$$V_2 = 0.60000$$

The angles of the inlet and exit velocity vectors were chosen as, respectively

$$\lambda_1 = 30.0000^\circ$$

$$\lambda_2 = 10.0000^\circ$$

## 360-Point Airfoil Design

The first step in the design of the 360-point airfoil in the cascade was the calculation of the velocity potential distribution by numerical integration of  $u(S)$ . Simpson's parabolic rule was used taking values of  $S$  in intervals of 0.025. The velocity potential distributions  $\phi_a(S)$  and  $u(S)$  are shown plotted jointly in figure 4. From the velocity potential,  $\Gamma$  was determined to be 0.28201 and  $\phi_{\min}$ , - 0.51556. The constants  $\lambda_m$ ,  $V_m$ , and  $d$  were calculated from equations (2), (3), and (5), respectively. The values obtained were as follows:  $\lambda_m = 20.6484^\circ$ ,  $V_m = 0.63144$ ,  $d = 1.19012$ .

The values of  $k$ ,  $\lambda_k$ ,  $\theta_N$ , and  $\theta_T$ , calculated by the trial-and-error process indicated in the numerical procedure, were found to be  $k = 0.48337$ ,  $\lambda_k = 9.6614^\circ$ ,  $\theta_N = -15.6038^\circ$ , and  $\theta_T = -183.7190^\circ$ , respectively.

The velocity distribution  $v_c(\theta)$  and the velocity potential distribution  $\phi_c(\theta)$  on the unit circle were calculated from equations (15) and (8), respectively. These distributions are shown plotted in figures 5 and 6, respectively.

The harmonic function  $p(\theta)$  was calculated from equation (17) and is shown plotted in figure 7.

In order to determine  $u(\theta)$ , the plot of  $\phi_a(S)$  was superimposed upon the plot of  $u(S)$  (fig. 4). Each value of  $\phi_c(\theta)$  (fig. 6) was then located on the  $\phi_a(S)$  curve and the  $u(S)$  value was read for the corresponding value of  $S$ . In this manner, the value of  $u(S)$  for a given  $\theta$ ,  $u(\theta)$ , could be directly determined.

In order to determine whether or not  $p(\theta)$  fulfilled the conditions on  $h(z)$ , the integrals

$$\int_{\theta_T}^{\theta_T + 2\pi} p(\theta) d\theta$$

$$\int_{\theta_T}^{\theta_T + 2\pi} p(\theta) \sin \theta \, d\theta$$

$$\int_{\theta_T}^{\theta_T + 2\pi} p(\theta) \cos \theta \, d\theta$$

were numerically integrated and the following values were obtained:

$$\int_{\theta_T}^{\theta_T + 2\pi} p(\theta) \, d\theta = 0.38236$$

$$\int_{\theta_T}^{\theta_T + 2\pi} p(\theta) \sin \theta \, d\theta = -0.09526$$

$$\int_{\theta_T}^{\theta_T + 2\pi} p(\theta) \cos \theta \, d\theta = 0.26919$$

In order to correct for airfoil closure, a function  $f(\theta)$  was formed such that

$$\int_{\theta_T}^{\theta_T + 2\pi} p'(\theta) \, d\theta = \int_{\theta_T}^{\theta_T + 2\pi} p'(\theta) \sin \theta \, d\theta = \int_{\theta_T}^{\theta_T + 2\pi} p'(\theta) \cos \theta \, d\theta = 0 \quad (19)$$

where

$$p'(\theta) = p(\theta) + f(\theta)$$

Initially,  $f(\theta)$  was assumed to be a function of the type given by equation (31). The wave lengths and zeros of the individual sine terms were picked somewhat arbitrarily except for the restriction that corrections on  $p(\theta)$  were to occur principally on the pressure surface. The amplitudes of the sine terms were then determined by the simultaneous solution of the equations

$$\int_{\theta_T}^{\theta_T + 2\pi} f(\theta) d\theta = - \int_{\theta_T}^{\theta_T + 2\pi} p(\theta) d\theta = - 0.38236$$

$$\int_{\theta_T}^{\theta_T + 2\pi} f(\theta) \cos \theta d\theta = - \int_{\theta_T}^{\theta_T + 2\pi} p(\theta) \cos \theta d\theta = - 0.26919$$

$$\int_{\theta_T}^{\theta_T + 2\pi} f(\theta) \sin \theta d\theta = - \int_{\theta_T}^{\theta_T + 2\pi} p(\theta) \sin \theta d\theta = 0.09526$$

Several other choices for the wave lengths and zeros of the sine terms were then made and the amplitudes for the terms were computed. The wave lengths and zeros that gave relatively small amplitudes for the terms were prescribed for the  $f(\theta)$  used for the correction. The function  $f(\theta)$  was defined in the interval  $\theta_T \leq \theta \leq \theta_T + 2\pi$  as follows:

$$f(\theta) = 0$$

for

$$- 183.719^\circ \leq \theta < - 176.281^\circ$$

$$f(\theta) = - 0.21488 \sin 7.5 (\theta + 176.281^\circ)$$



for

$$-176.281^\circ \leq \theta < -157.5^\circ$$

$$f(\theta) = -0.21488 \sin 7.5 (\theta + 176.281^\circ) + 0.008703 \sin 4/3 (\theta + 157.5^\circ)$$

for

$$-157.5^\circ \leq \theta < -152.281^\circ$$

$$f(\theta) = 0.008703 \sin 4/3 (\theta + 157.5^\circ)$$

for

$$-152.281^\circ \leq \theta < -27.719^\circ$$

$$f(\theta) = 0.008703 \sin 4/3 (\theta + 157.5^\circ) - 1.26792 \sin 7.5 (\theta + 27.719^\circ)$$

for

$$-27.719^\circ \leq \theta < -22.5^\circ$$

$$f(\theta) = -1.26792 \sin 7.5 (\theta + 27.719^\circ)$$

for

$$-22.5^\circ \leq \theta < -3.719^\circ$$

$$f(\theta) = 0$$

for

$$-3.719^\circ \leq \theta \leq 176.281^\circ$$

Graphically,  $f(\theta)$  plotted in figure 7, consisted of the sum of three separate sine loops. The curve  $p'(\theta) = p(\theta) + f(\theta)$  is shown plotted in figure 8.

The corrected velocity  $v'(\theta)$  and the corrected arc length  $S'(\theta)$  were computed from equations (20) and (21), respectively. The corrected-velocity distribution  $v'(S')$  is shown plotted in figure 9. This velocity distribution is the actual distribution for the computed airfoil shape. The peak on the suction surface in the nose region is undesirable, but steps were not taken to correct it in the present example.

The values of  $p'(\theta)$  at the  $1^\circ$  intervals were used to calculate the conjugate harmonic function  $q(\theta)$  (fig. 10) by use of the method outlined by Naiman (reference 6). The actual computation of this function was performed on punch-card machines. Interpolation was necessary to find the values of  $q(\theta)$  as the preceding method gave values of  $q(\theta - 1/2^\circ)$ .

The values of  $q(\theta)$  were used to compute  $\beta(\theta)$  from equation (25) and the coordinates of an airfoil in the cascade from equations (26) and (27) (numerical integration). The resulting airfoil is shown in figure 11.

### 90-Point Airfoil Design

The computations for the 90-point design remained the same as in the previous case, in that the chosen 90 points were taken from the 360 points except that the function  $p(\theta)$  had to be recorrected for closure. Recorrection was necessary because of the discrepancy in the numerical integration used, as the integration was performed over larger intervals. The corrections for closure were made within the limits chosen in the previous case. The resulting function  $p'(\theta)$  is shown in figure 12.

The conjugate harmonic function  $q(\theta)$  was computed from  $p'(\theta)$  using the 90-point method of Naiman (reference 6) and is shown in figure 13. The airfoil coordinates were computed and the resulting profile is shown in figure 14. It is seen that this airfoil is crossed near the trailing edge and remains open at the trailing edge.

### Comparison of 360- and 90-Point Airfoils

It can be seen from equations (25), (26), and (27) that a change in  $q(\theta)$  would introduce a change in the values of the integrands in equations (26) and (27) and, consequently, would introduce a change in the final airfoil coordinates. Hence, the fact that the 90-point airfoil remained open although the conditions for closure were satisfied could possibly be attributed to the fact that the 90-point method of Naiman did not insure sufficient accuracy in the values of  $q(\theta)$  for the present example. This possibility was therefore investigated.

In order to increase the accuracy of  $q(\theta)$ , it was decided to use the 360-point method of Naiman. In order to obtain the 360 values of  $p'(\theta)$  necessary for the computation, parabolic interpolation was

used. This type of interpolation was used because the integration of  $p'(\theta)$  by Simpson's 1/3 rule in satisfying closure requirements had already assumed a parabolic variation between the values of  $p'(\theta)$ . The interpolated values were then used to derive new values of  $q(\theta)$  at the chosen 90 points, and the airfoil coordinates were then computed. The new profile, shown in figure 15, has a closed contour. The slight variation between the shape of this airfoil and the original 360-point airfoil (fig. 11) can be attributed to the integration of equations (26) and (27) over larger intervals and the recorection of  $p(\theta)$  for closure.

An investigation was also made to determine, if possible, in what manner and in what regions the change in  $q(\theta)$  influenced the integrands of equations (26) and (27). In order to make this determination, the following calculations were made and plotted: the difference in the values of  $q(\theta)$ , as obtained from the 360-point and 90-point methods of Naiman (fig. 16); the differences in  $q(\theta)$  divided by  $Q(\theta)$ ; and the differences in the integrands of equations (26) and (27); as obtained by using the values of  $q(\theta)$  derived from the two different methods. A plot of the differences in the integrand of equation (26) was superimposed upon a plot of the difference in  $q(\theta)/Q(\theta)$  (fig. 17). A similar plot was made for equation (27) (fig. 18).

The differences in  $q(\theta)/Q(\theta)$  show a definite correlation to the differences in the integrands in equations (26) and (27), as  $q(\theta)$  enters into the expression for  $\beta(\theta)$  as  $q(\theta)/Q(\theta)$ . It should be noted that the changes in  $q(\theta)/Q(\theta)$  seem to have the least influence on the integrands in the vicinity of  $\theta_N$  ( $-15.6038^\circ$ ).

### CONCLUSIONS

It can be concluded from the comparison of the 90- and 360-point airfoils that the 90-point method of Naiman does not insure sufficient accuracy in values of the conjugate function  $q(\theta)$  for all cases, as shown by the numerical example presented. The accuracy of Naiman's method will depend on the shape of the harmonic function  $p(\theta)$ , which in turn depends on the design conditions prescribed. As a consequence, it is not to be inferred that Naiman's method, applied to 90 points or less, will not give accurate results for most cases.

Lewis Flight Propulsion Laboratory,  
National Advisory Committee for Aeronautics,  
Cleveland, Ohio, September 15, 1949..

## REFERENCES

1. Weinig, F.: Die Strömung um die Schaufeln von Turbomaschinen. Johann-Ambrosius Barth (Leipzig), 1935.
2. Mutterperl, William: A Solution of the Direct and Inverse Potential Problems for Arbitrary Cascades of Airfoils. NACA ARR L4K22b, 1944.
3. Lighthill, M. J.: A Mathematical Method of Cascade Design. R. & M. No. 2104, British A.R.C., June 1945.
4. Garrick, I. E.: On the Plane Potential Flow past a Lattice of Arbitrary Airfoils. NACA Rep. 788, 1944.
5. Goldstein, Arthur, and Jerison, Meyer: Isolated and Cascade Airfoils with Prescribed Velocity Distributions. NACA Rep. 869, 1947. (pp. 23-24)
6. Naiman, Irven: Numerical Evaluation by Harmonic Analysis of the  $\epsilon$ -Function of the Theodorsen Arbitrary-Airfoil Potential Theory. NACA ARR L5H18, 1945.

1242

TABLE I - OUTLINE FOR COMPUTATION OF  $k$ 

	Definition	Operation	Remarks
	$k$	Assumed	
1	$\sinh k$	$\sinh k$	
2	$\cosh k$	$\cosh k$	
3	$\tanh k$	$\tanh k$	
4	$\sin \lambda_m$	$\sin \lambda_m$	
5	$\cos \lambda_m$	$\cos \lambda_m$	
6	$\tan \lambda_m$	$\tan \lambda_m$	
7	$\tan \lambda_k$	$(6) \times (3)$	
8	$\lambda_k$	$\tan^{-1} (7)$	$-\frac{\pi}{2} \leq \lambda_k \leq \frac{\pi}{2}$
9	$\sin \lambda_k$	$\sin (8)$	
10	$\sin (\theta_N + \lambda_k)$	$\left[ \frac{-\Gamma}{2V_\infty d} \times (2) \times (9) \right] / (4)$	
11	$\theta_N + \lambda_k$	$\sin^{-1} (10)$	$-\frac{\pi}{2} \leq \theta_N + \lambda_k \leq \frac{\pi}{2}$
12	$\theta_N$	$(11) - (8)$	
13	$\theta_T$	$-(12) - 2(8) - 180^\circ$	
14	$\sin \theta_N$	$\sin (12)$	
15	$\cos \theta_N$	$\cos (12)$	
16	$\tan \theta_N$	$\tan (12)$	
17	$\sin \theta_T$	$\sin (13)$	
18	$\cos \theta_T$	$\cos (13)$	
19	$\tan \theta_T$	$\tan (13)$	
20	$\sin \theta_T / \sinh k$	$(17)/(1)$	
21	$\sin \theta_N / \sinh k$	$(14)/(1)$	
22	$\cos \theta_T / \cosh k$	$(18)/(2)$	
23	$\cos \theta_N / \cosh k$	$(15)/(2)$	



TABLE I - OUTLINE FOR COMPUTATION OF  $k$  - Concluded

	Definition	Operation	Remarks
24	$\tan \theta_T / \tanh k$	(19)/(3)	
25	$\tan \theta_N / \tanh k$	(16)/(3)	
26	$\tan^{-1} \left( \frac{\sin \theta_T}{\sinh k} \right)$	$\tan^{-1} (20)$	Express in radians $-\frac{\pi}{2} \leq \tan^{-1} \left( \frac{\sin \theta_T}{\sinh k} \right) \leq \frac{\pi}{2}$
27	$\tan^{-1} \left( \frac{\sin \theta_N}{\sinh k} \right)$	$\tan^{-1} (21)$	Express in radians $-\frac{\pi}{2} \leq \tan^{-1} \left( \frac{\sin \theta_N}{\sinh k} \right) \leq \frac{\pi}{2}$
28	$\tanh^{-1} \left( \frac{\cos \theta_T}{\cosh k} \right)$	$\tanh^{-1} (22)$	
29	$\tanh^{-1} \left( \frac{\cos \theta_N}{\cosh k} \right)$	$\tanh^{-1} (23)$	
30	$\tan^{-1} \left( \frac{\tan \theta_T}{\tanh k} \right)$	$\tan^{-1} (24)$	Express in radians; same quadrant and sign as $\theta_T$
31	$\tan^{-1} \left( \frac{\tan \theta_N}{\tanh k} \right)$	$\tan^{-1} (25)$	Express in radians; same quadrant and sign as $\theta_N$
32	$\sin \lambda_m \left[ \tan^{-1} \left( \frac{\sin \theta_T}{\sinh k} \right) - \tan^{-1} \left( \frac{\sin \theta_N}{\sinh k} \right) \right]$	(4) [(26) - (27)]	
33	$\cos \lambda_m \left[ \tanh^{-1} \left( \frac{\cos \theta_T}{\cosh k} \right) - \tanh^{-1} \left( \frac{\cos \theta_N}{\cosh k} \right) \right]$	(5) [(28) - (29)]	
34	$\frac{\Gamma}{2V_m d} \left[ \tan^{-1} \left( \frac{\tan \theta_T}{\tanh k} \right) - \tan^{-1} \left( \frac{\tan \theta_N}{\tanh k} \right) + 2\pi \right]$	$\frac{\Gamma}{2V_m d} [(30) - (31) + 6.2832]$	
35		(32) - (33) + (34)	
36	$\Delta_k$	$\frac{V_m d}{\pi} \times (35)$	This result must equal $\Gamma - \phi_{\min}$ for correct value for $k$

TABLE II - OUTLINE FOR COMPUTATION OF AIRFOIL COORDINATES

	Definition	Operation	Remarks
	$\theta$	Assign in equal intervals	$\theta_T \leq \theta \leq \theta_T + 2\pi$
1	$2\theta$	$2\theta$	
2	$\cos 2\theta$	$\cos (1)$	
3	$\cosh 2k - \cos 2\theta$	$\cosh 2k - (2)$	
4	$Q(\theta) = \frac{\sinh 2k}{\cosh 2k - \cos 2\theta}$	$\frac{\sinh 2k}{(3)}$	
5	$\theta + \lambda_k$	$\theta + \lambda_k$	
6	$\sin (\theta + \lambda_k)$	$\sin (5)$	
7	$\sin (\theta + \lambda_k) - \sin (\theta_N + \lambda_k)$	$(6) - \sin (\theta_N + \lambda_k)$	
8	$\left[ \frac{V_m d \sin \lambda_m}{\pi \sin \lambda_k \cosh k} \right] \times$ $[\sin (\theta + \lambda_k) - \sin (\theta_N + \lambda_k)]$	$\frac{V_m d \sin \lambda_m}{\pi \sin \lambda_k \cosh k} \times (7)$	
9	$v_c (\theta)$	$(8) \times (4)$	
10	$\sin \theta$	$\sin \theta$	
11	$\cos \theta$	$\cos \theta$	
12	$\tan \theta$	$\tan \theta$	
13	$\sin \theta / \sinh k$	$(10) / \sinh k$	
14	$\cos \theta / \cosh k$	$(11) / \cosh k$	
15	$\tan \theta / \tanh k$	$(12) / \tanh k$	
16	$\tan^{-1} \left( \frac{\sin \theta}{\sinh k} \right)$	$\tan^{-1} (13)$	Express in radians $-\frac{\pi}{2} \leq \tan^{-1} \left( \frac{\sin \theta}{\sinh k} \right) \leq \frac{\pi}{2}$
17	$\tanh^{-1} \left( \frac{\cos \theta}{\cosh k} \right)$	$\tanh^{-1} (14)$	
18	$\tan^{-1} \left( \frac{\tan \theta}{\tanh k} \right)$	$\tan^{-1} (15)$	Express in radians $\tan^{-1} \left( \frac{\tan \theta}{\tanh k} \right)$ is in the same quadrant and of the same sign as $\theta$

NACA

TABLE II - OUTLINE FOR COMPUTATION OF AIRFOIL COORDINATES - Continued

	Definition	Operation	Remarks
35		$C_1 - k - (33) - (34)$	$C_1 = \log_e \sqrt{2(\cosh 2k - \cos 2\theta_T)}$
36		$\left(\frac{1}{2} - \frac{\epsilon}{2\pi}\right) \times (35)$	$\epsilon = \pi$ for rounded tail $\epsilon = 0$ for cusped tail
37		$(32) + k + (36)$	
38	$p(\theta)$	$(4) \times (37)$	
39	$p(\theta) \sin \theta$	$(38) \times (10)$	
40	$p(\theta) \cos \theta$	$(38) \times (11)$	
41	$\int_{\theta_T}^{\theta_T+2\pi} p(\theta) d\theta$	$\int_{\theta_T}^{\theta_T+2\pi} (38) d\theta$	
42	$\int_{\theta_T}^{\theta_T+2\pi} p(\theta) \sin \theta d\theta$	$\int_{\theta_T}^{\theta_T+2\pi} (39) d\theta$	
43	$\int_{\theta_T}^{\theta_T+2\pi} p(\theta) \cos \theta d\theta$	$\int_{\theta_T}^{\theta_T+2\pi} (40) d\theta$	
44	$f(\theta)$	Assigned arbitrarily	See Numerical Procedure
45	$p'(\theta) = p(\theta) + f(\theta)$	$(38) + (44)$	
46	$p'(\theta) \sin \theta$	$(45) \times (10)$	
47	$p'(\theta) \cos \theta$	$(45) \times (11)$	
48	$\int_{\theta_T}^{\theta_T+2\pi} p'(\theta) d\theta$	$\int_{\theta_T}^{\theta_T+2\pi} (45) d\theta$	Must be equal to zero
49	$\int_{\theta_T}^{\theta_T+2\pi} p'(\theta) \sin \theta d\theta$	$\int_{\theta_T}^{\theta_T+2\pi} (46) d\theta$	Must be equal to zero



TABLE II - OUTLINE FOR COMPUTATION OF AIRFOIL COORDINATES - Continued

	Definition	Operation	Remarks
19	$\sin \lambda_m \tan^{-1} \left( \frac{\sin \theta}{\sinh k} \right)$	$\sin \lambda_m \times (16)$	
20	$\cos \lambda_m \tanh^{-1} \left( \frac{\cos \theta}{\cosh k} \right)$	$\cos \lambda_m \times (17)$	
21	$\frac{\Gamma}{2V_m d} \tan^{-1} \left( \frac{\tan \theta}{\tanh k} \right)$	$\frac{\Gamma}{2V_m d} \times (18)$	
22		$(19) - (20) + (21)$	
23		$\frac{V_m d}{\pi} \times (22)$	
24	$\varphi_c(\theta)$	$(23) - C_7$	$C_7$ is the first value given in column (23)
25	$u(\theta)$	$(24)$ and curve reading	
26	$\frac{\pi}{dQ(\theta)}$	$\frac{\pi}{d}/(4)$	
27	$\frac{\pi V_c(\theta)}{dQ(\theta) u(\theta)}$	$[(26) \times (9)]/(25)$	
28	$\frac{\theta - \theta_T}{2}$	$\frac{\theta - \theta_T}{2}$	
29	$2 \sin \left( \frac{\theta - \theta_T}{2} \right)$	$2 \sin (28)$	
30	$\left[ 2 \sin \left( \frac{\theta - \theta_T}{2} \right) \right]^{\left( \frac{\epsilon}{\pi} - 1 \right)}$	$\left( \frac{\epsilon}{\pi} - 1 \right)$ (29)	$\epsilon = \pi$ for rounded tail $\epsilon = 0$ for cusped tail
31		$(27) \times (30)$	
32		$\log_e (31)$	
33		$e^k \tan^{-1} \left( \frac{\sin \theta_T}{\sinh k} \right) \times (10)$	
34		$e^k \tanh^{-1} \left( \frac{\cos \theta_T}{\cosh k} \right) \times (11)$	

TABLE II - OUTLINE FOR COMPUTATION OF AIRFOIL COORDINATES - Continued

	Definition	Operation	Remarks
50	$\int_{\theta_T}^{\theta_T+2\pi} p'(\theta) \cos \theta \, d\theta$	$\int_{\theta_T}^{\theta_T+2\pi} (47) \, d\theta$	Must be equal to zero
51	$q(\theta)$	Conjugate harmonic function of (45)	
52	$f(\theta)/q(\theta)$	(44)/(4)	
53	$e^{-\frac{f(\theta)}{q(\theta)}}$	$e^{-(52)}$	
54	$u'(\theta) = u(\theta) e^{-\frac{f(\theta)}{q(\theta)}}$	(25) $\times$ (53)	
55	$\tan^{-1} \left( \frac{\sin \theta_T}{\sinh k} \right) \cos \theta$	$\tan^{-1} \left( \frac{\sin \theta_T}{\sinh k} \right) \times (11)$	
56	$\tanh^{-1} \left( \frac{\cos \theta_T}{\cosh k} \right) \sin \theta$	$\tanh^{-1} \left( \frac{\cos \theta_T}{\cosh k} \right) \times (10)$	
57		(55) - (56)	
58		$\frac{e^k}{2} \times (57)$	
59	$\theta(\text{radians})$	$\theta(\text{deg}) \times \frac{\pi}{180}$	
60	$\frac{\theta}{2}(\text{radians})$	(59)/2	
61		$c_2 - (60) + (58)$	$c_2 = \frac{\pi}{2} + \frac{1}{2} \tan^{-1} \left( \frac{\tan \theta_T}{\tanh k} \right)$
62		$\left(1 - \frac{\epsilon}{\pi}\right) \times (61)$	$\epsilon = \pi$ for rounded tail $\epsilon = 0$ for cusped tail
63	$q(\theta)/q(\theta)$	(51)/(4)	
64	$\beta(\theta)$	(63) + (62) + (59) + $\frac{\pi}{2}$	Radians
65	$\cos \beta(\theta)$	$\cos (64)$	

TABLE II - OUTLINE FOR COMPUTATION OF AIRFOIL COORDINATES - Concluded

	Definition	Operation	Remarks
66	$\sin \beta(\theta)$	$\sin (64)$	
67	$\frac{v_c(\theta)}{u'(\theta)}$	$(9)/(54)$	
68	$\frac{v_c(\theta)}{u'(\theta)} \cos \beta(\theta)$	$(67) \times (65)$	
69	$\frac{v_c(\theta)}{u'(\theta)} \sin \beta(\theta)$	$(67) \times (66)$	
70	$\xi - \xi_T$ $= \int_{\theta_T}^{\theta} \frac{v_c(\theta)}{u'(\theta)} \cos \beta(\theta) d\theta$	$\int_{\theta_T}^{\theta} (68) d\theta$	
71	$\eta - \eta_T$ $= \int_{\theta_T}^{\theta} \frac{v_c(\theta)}{u'(\theta)} \sin \beta(\theta) d\theta$	$\int_{\theta_T}^{\theta} (69) d\theta$	


 NACA

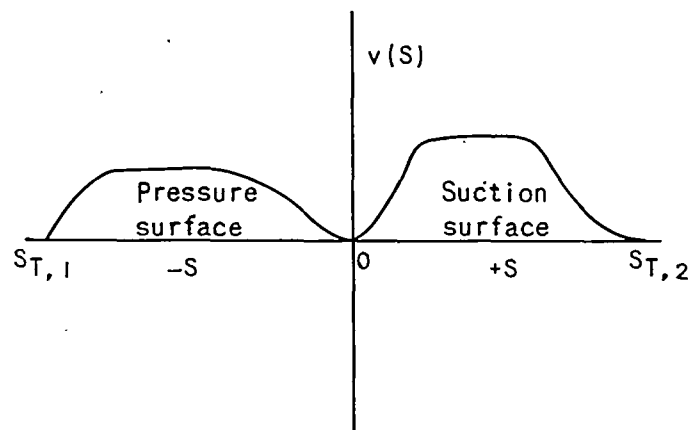


Figure 1. - Velocity distribution.

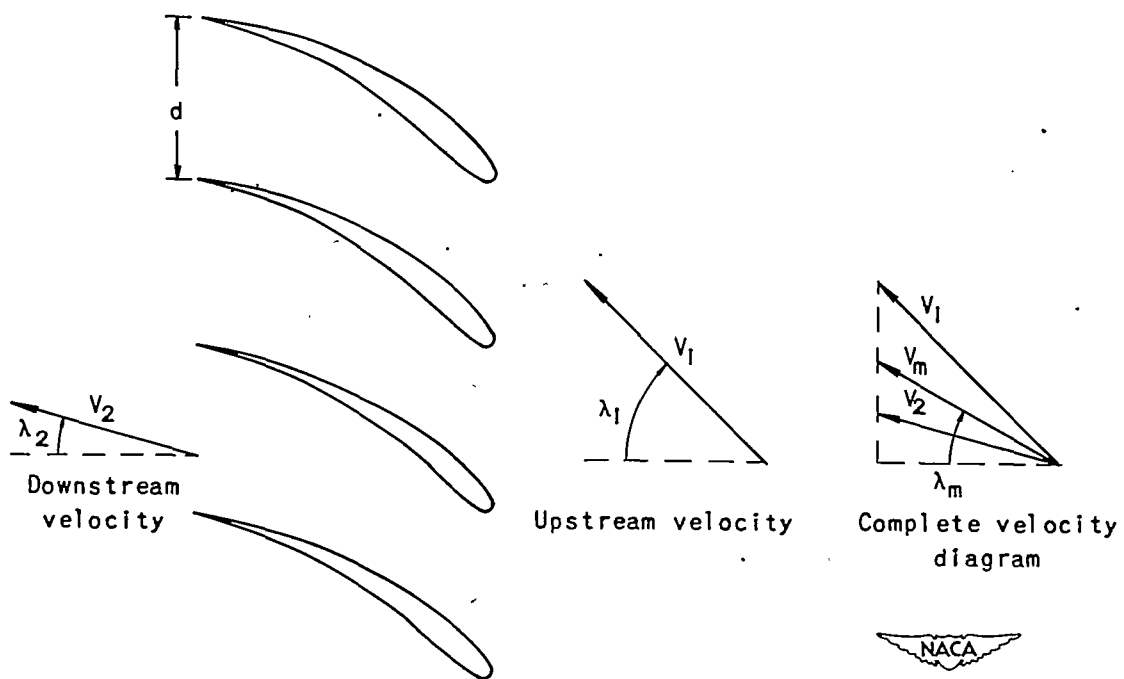


Figure 2. - Notation for cascade flow.

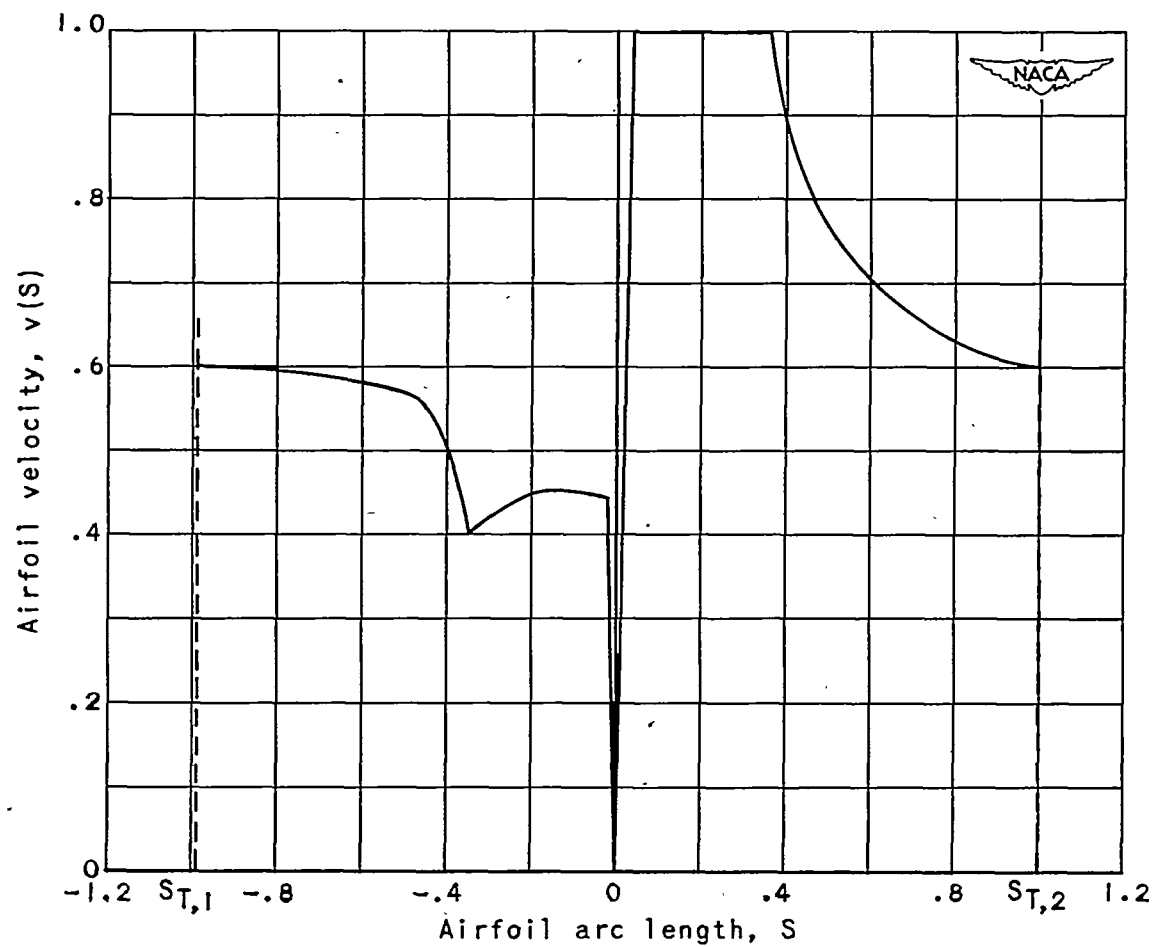


Figure 3. - Prescribed velocity distribution on airfoil.

1242

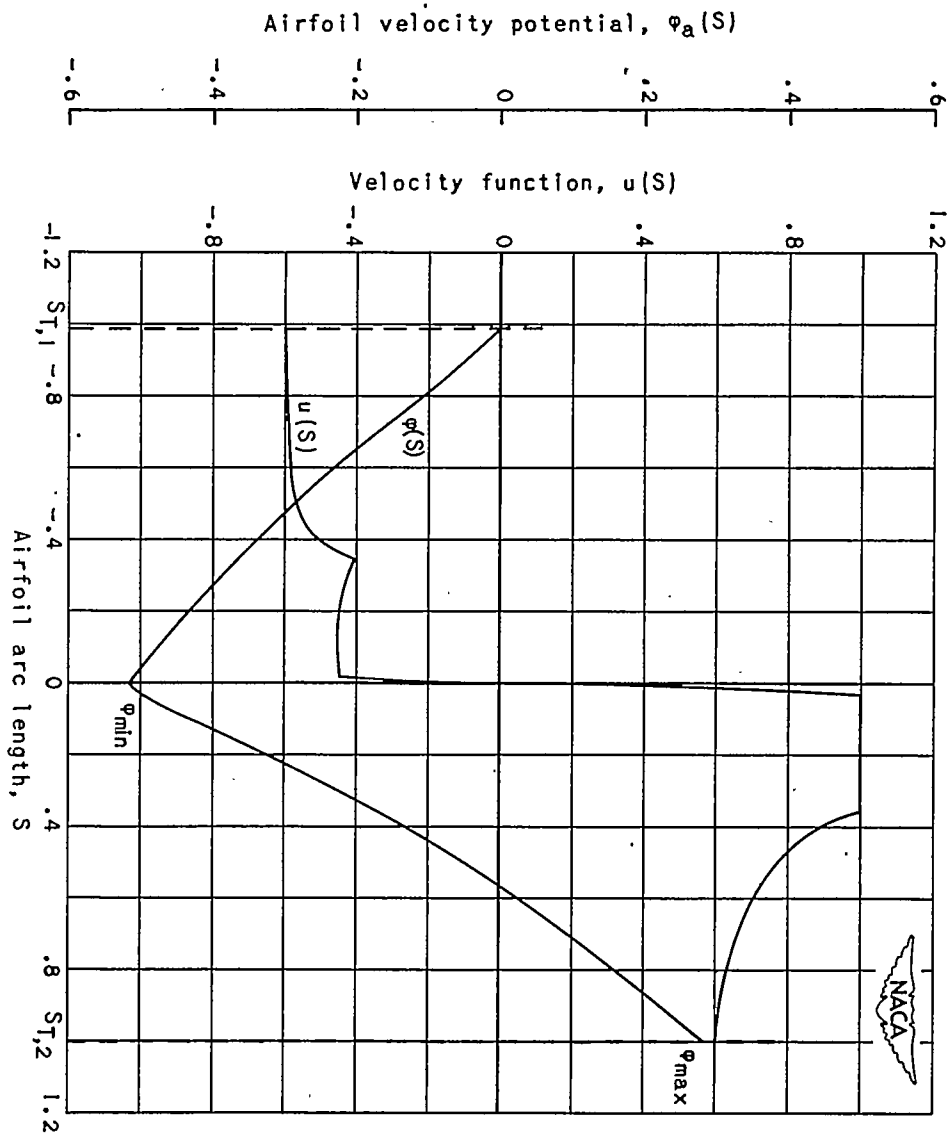


Figure 4. - Velocity function  $u(S)$  on airfoil and velocity potential distribution on airfoil.

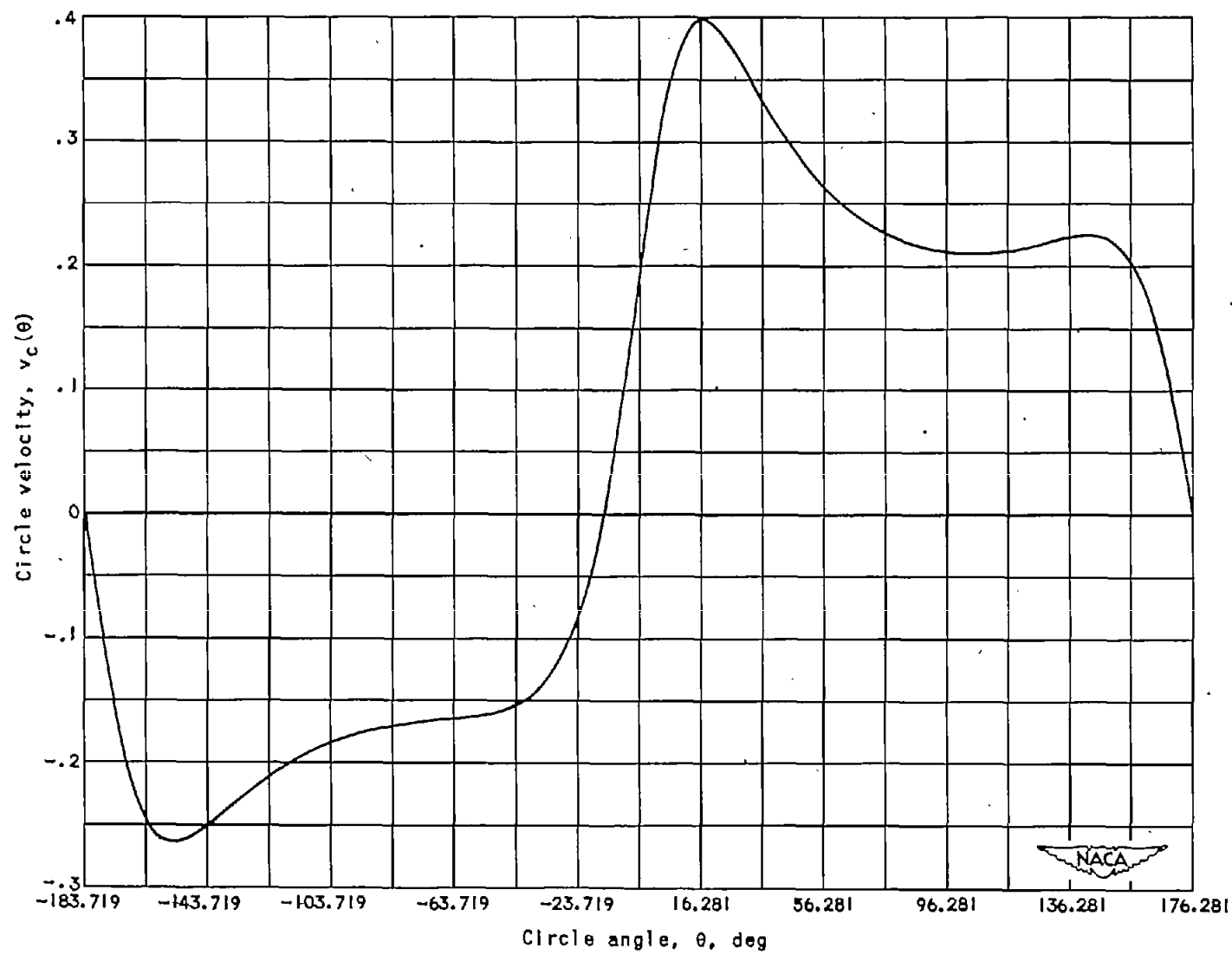


Figure 5. - Velocity distribution on unit circle.

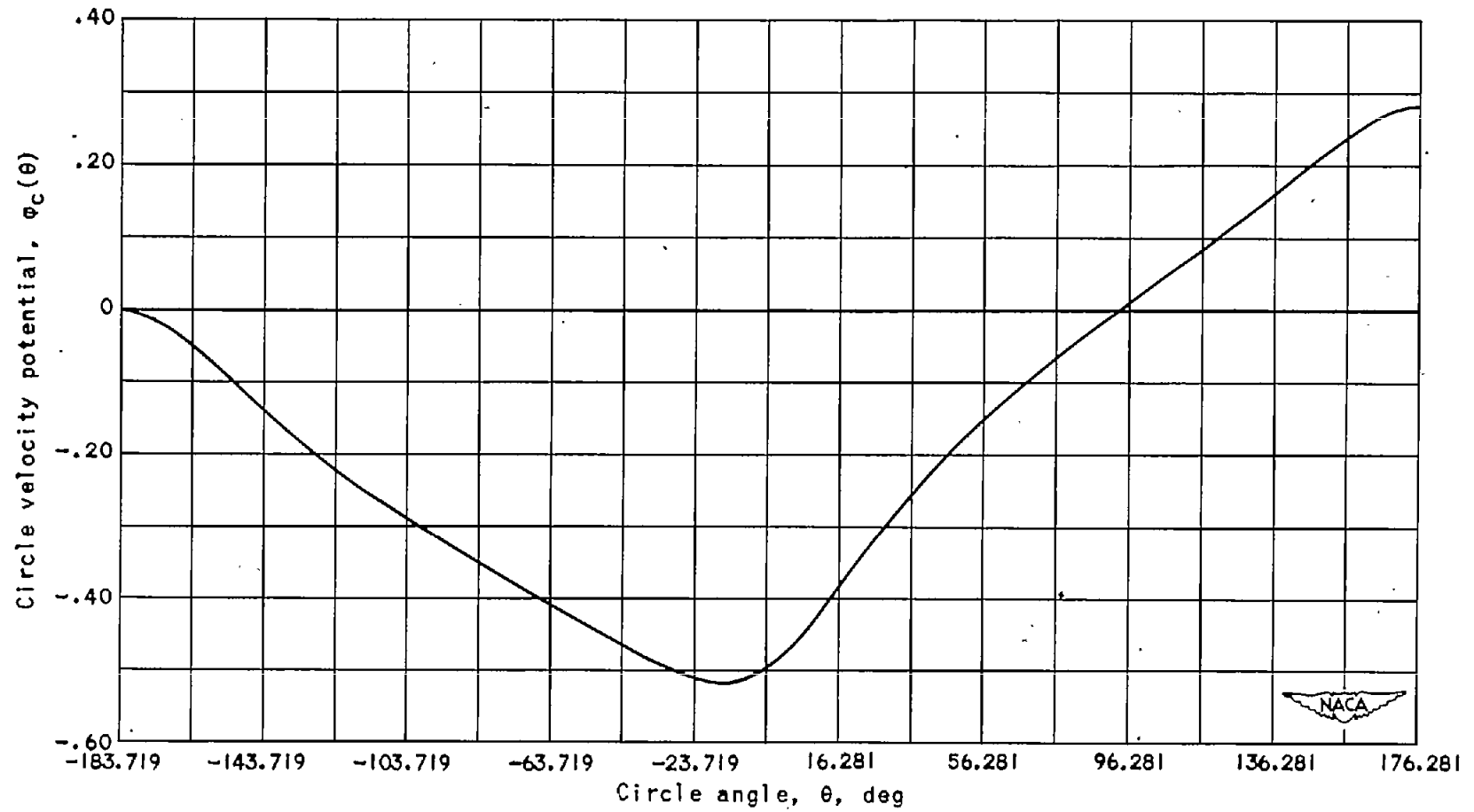


Figure 6. - Velocity-potential distribution on unit circle.



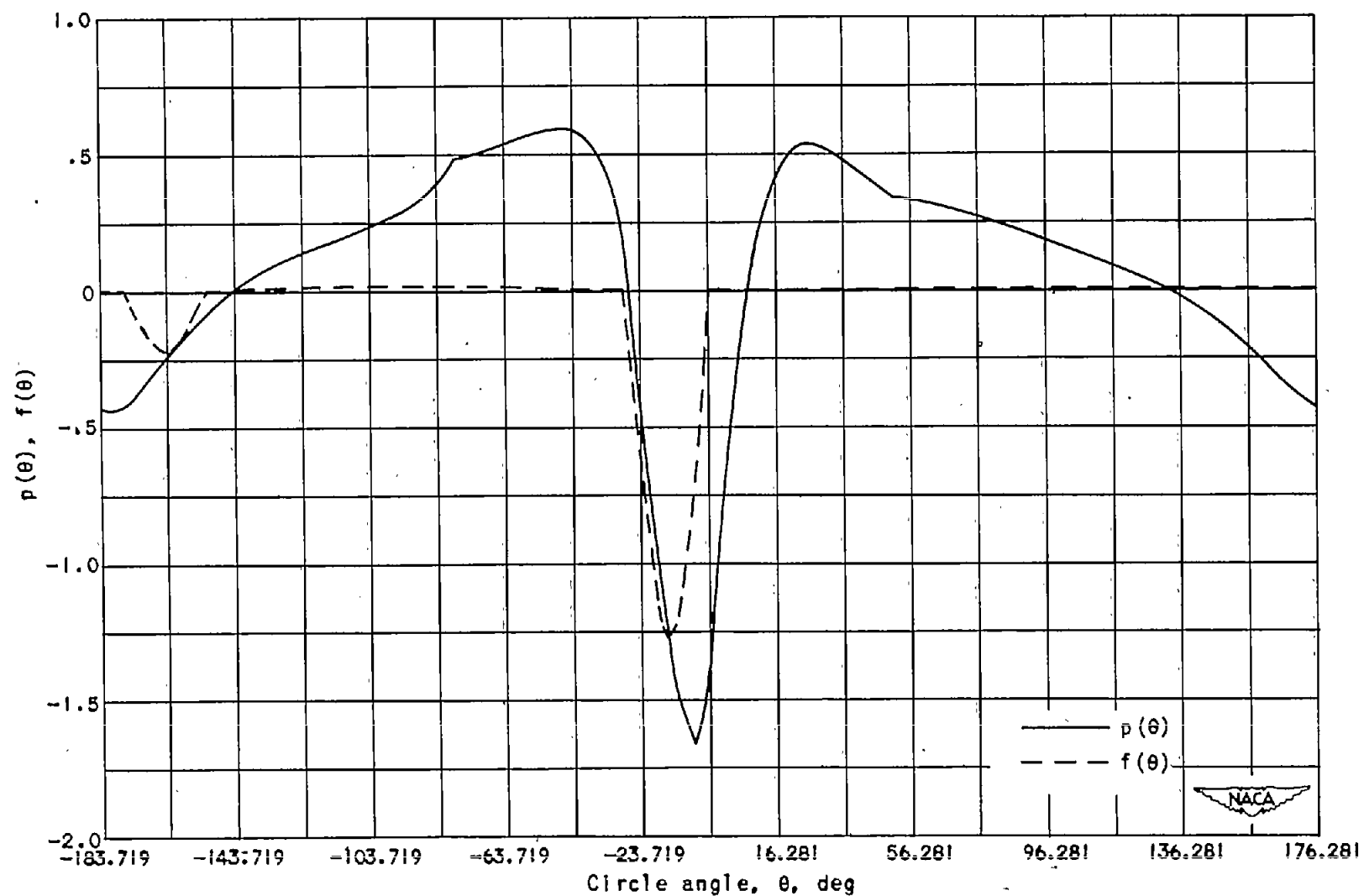


Figure 7. - Harmonic function  $p(\theta)$  and correction function  $f(\theta)$ , computed for 360 points.

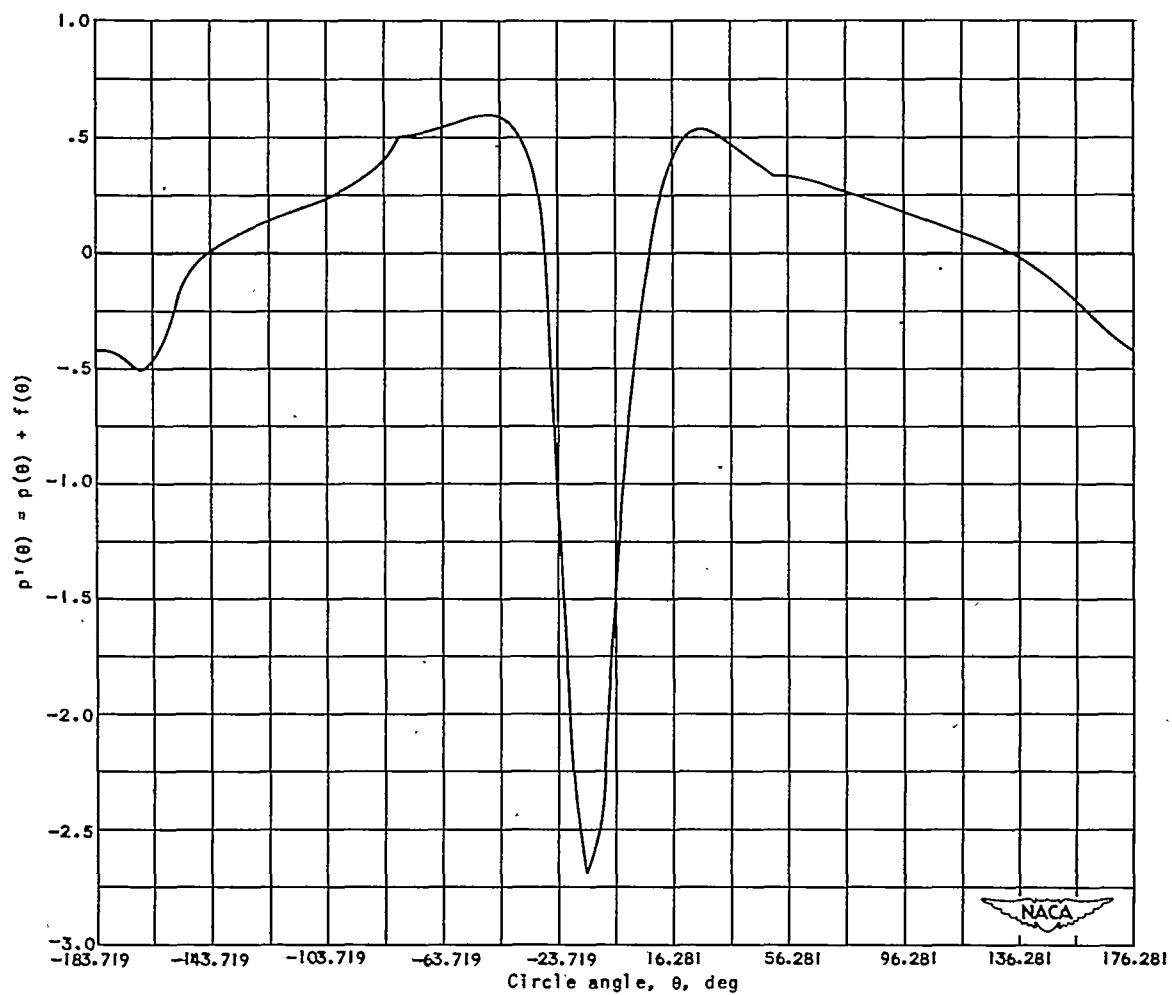


Figure 8. - Corrected harmonic function  $p'(\theta)$ , computed for 360 points.

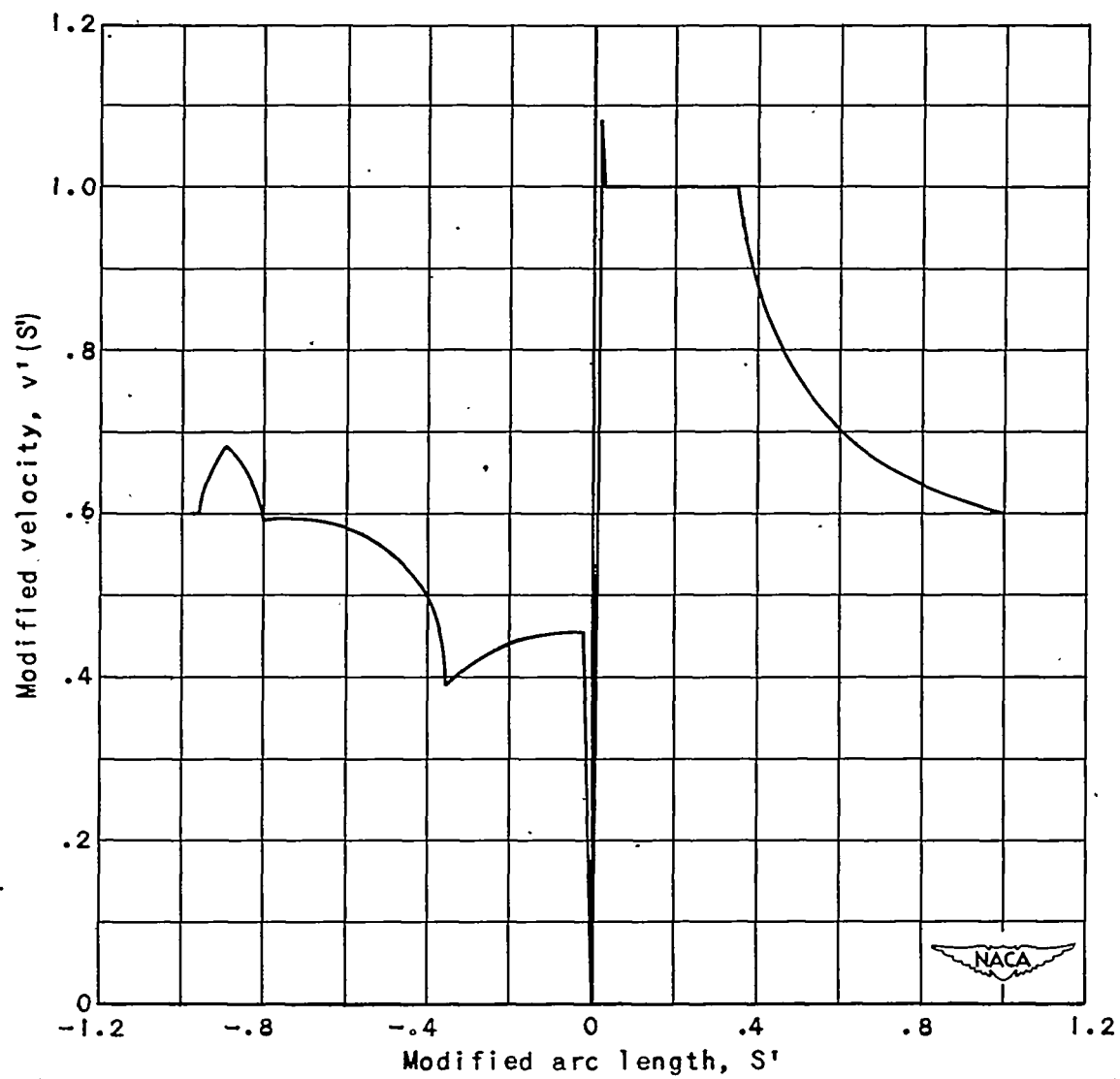


Figure 9. - Modified velocity distribution on airfoil.

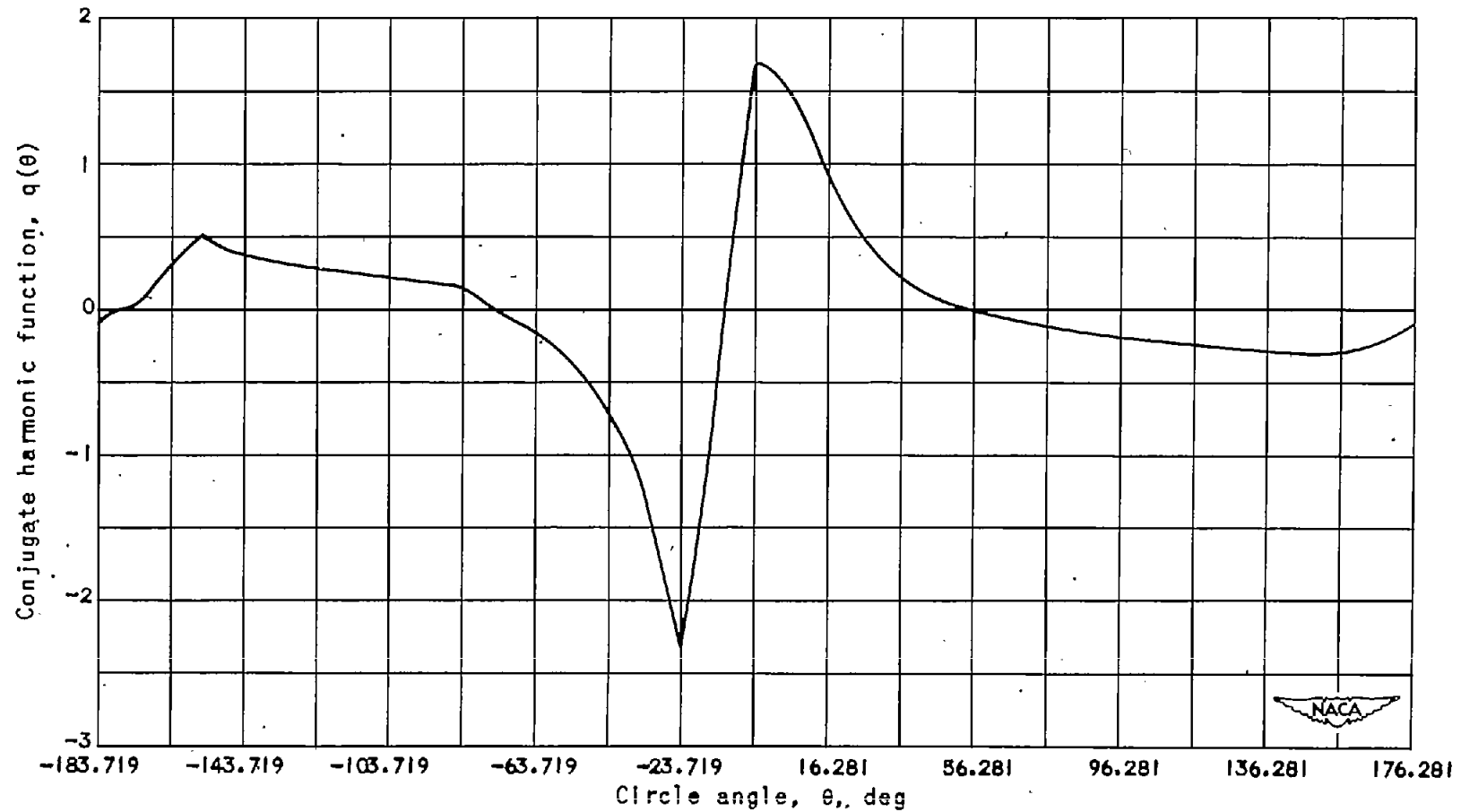


Figure 10. - Conjugate harmonic function  $q(\theta)$ , computed for 360 points.

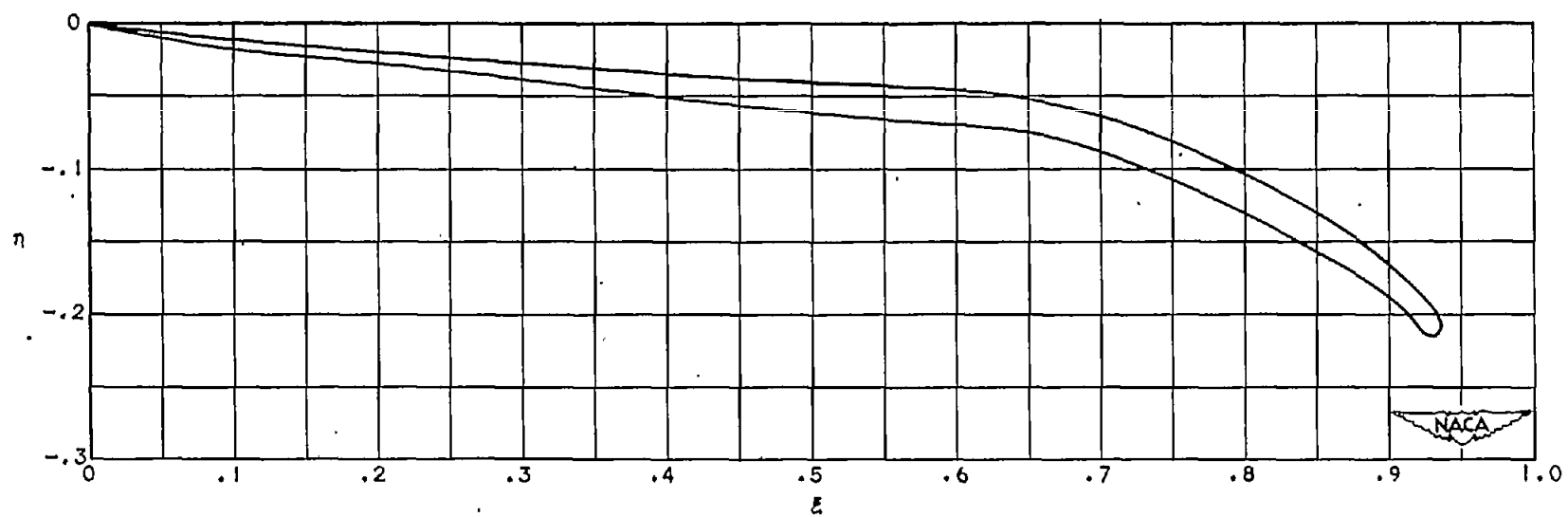


Figure 11. - Airfoil computed from 360 points.

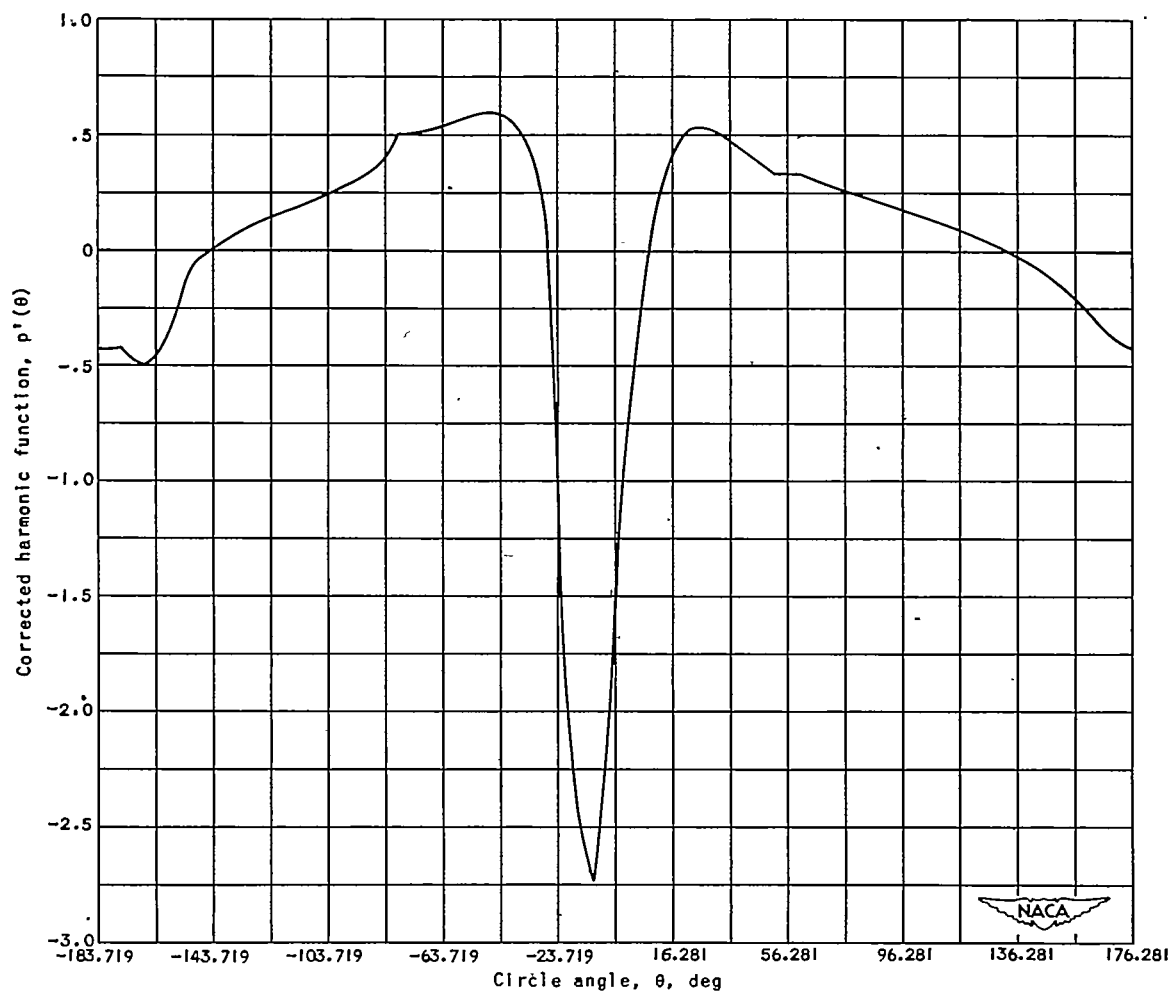


Figure 12. - Harmonic function  $p'(\theta)$  corrected for 90 points.

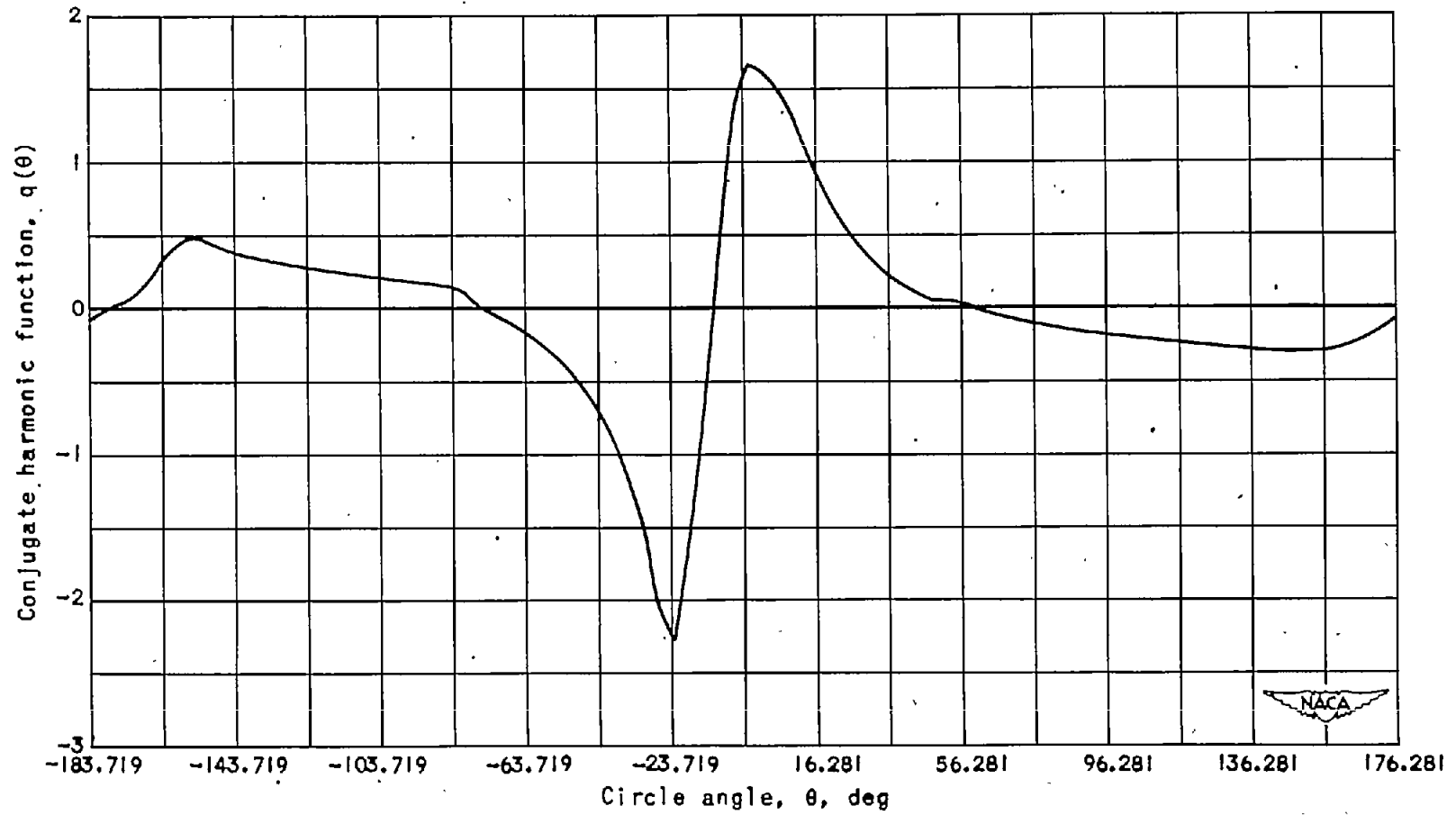


Figure 13. - Conjugate harmonic function  $q(\theta)$ , computed from 90 points.

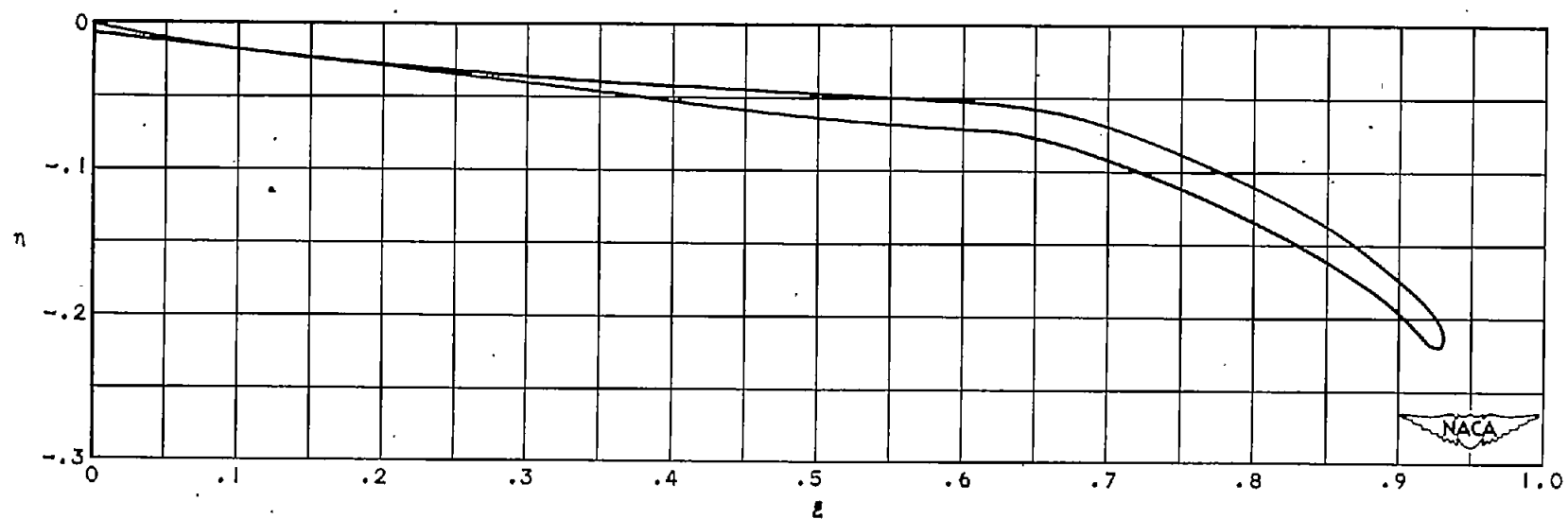


Figure 14. - Airfoil computed from 90 points.



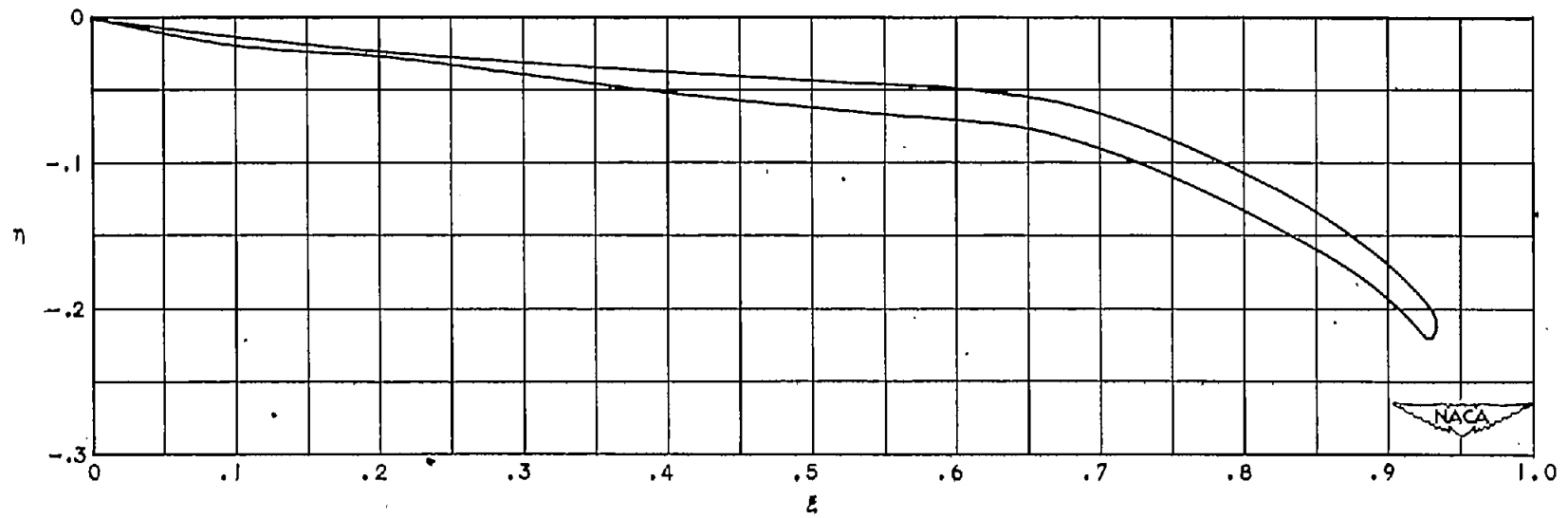


Figure 15. - 90-point airfoil computed from 360-point  $q(\theta)$ .

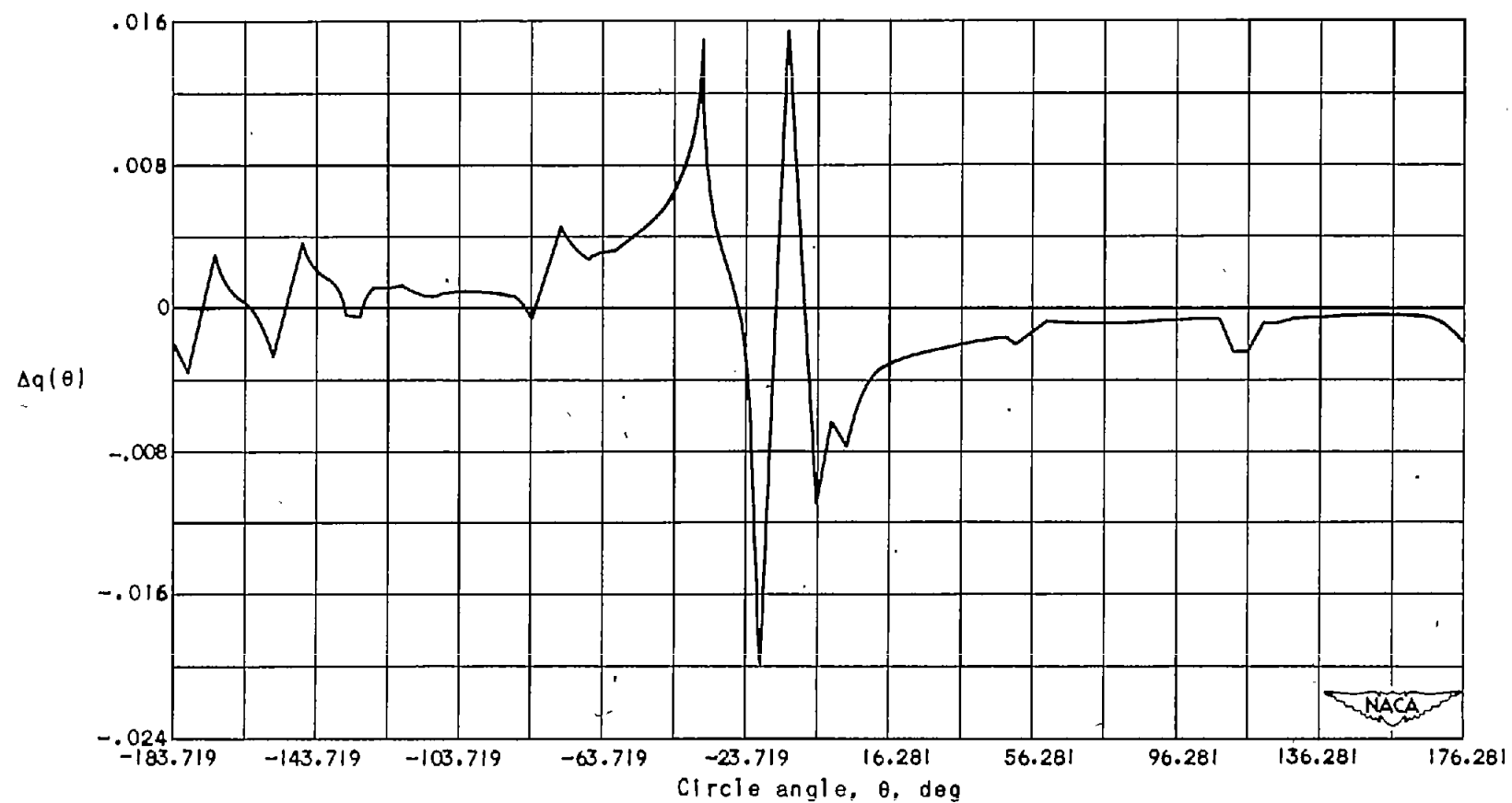


Figure 16. - Differences between 36Q-point  $q(\theta)$  and 90-point  $q(\theta)$ .

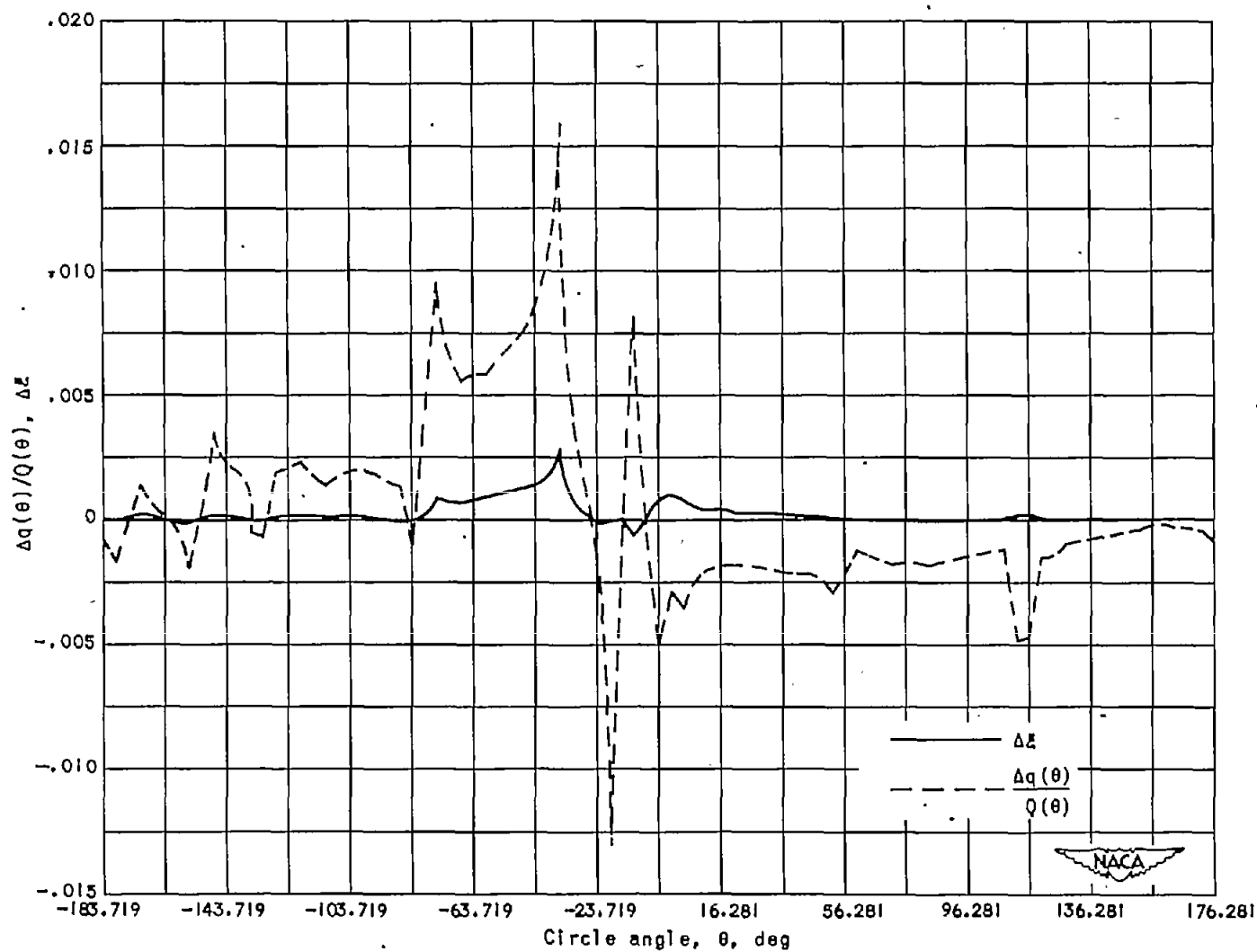


Figure 17. - Differences in 360-point  $q(\theta)$  and 90-point  $q(\theta)$ , divided by  $Q(\theta)$ ; differences in  $\Delta$  integrand from 360-point  $q(\theta)$  and 90-point  $q(\theta)$ .

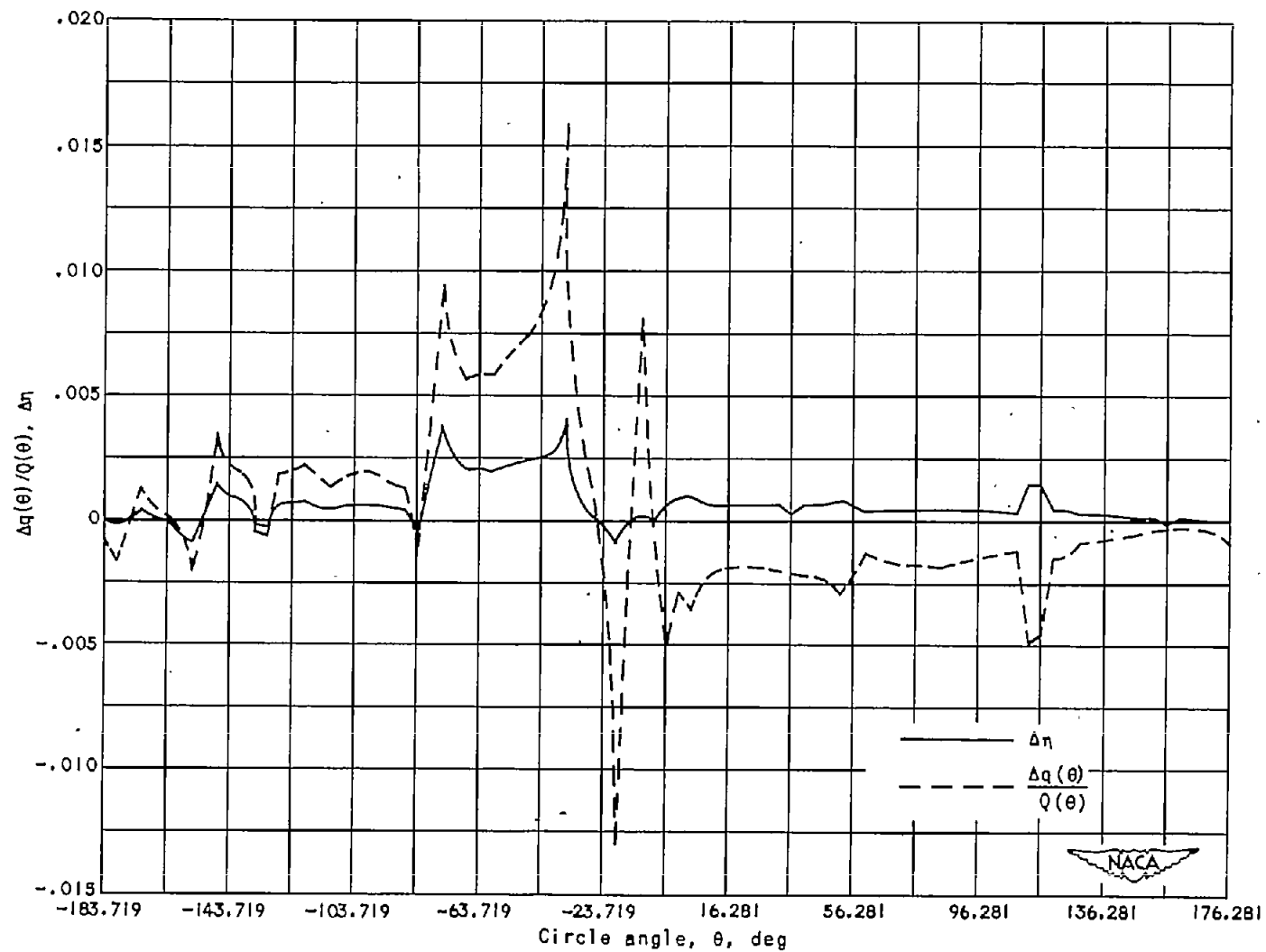


Figure 18. - Differences in 360-point  $q(\theta)$  and 90-point  $q(\theta)$ , divided by  $Q(\theta)$ ; differences in  $\eta$  integrand from 360-point  $q(\theta)$  and 90-point  $q(\theta)$ .